Adaptive Neural Control for a Class of Nonlinear Systems With Uncertain Hysteresis Inputs and Time-Varying State Delays

Beibei Ren, *Student Member, IEEE*, Shuzhi Sam Ge, *Fellow, IEEE*, Tong Heng Lee, *Member, IEEE*, and Chun-Yi Su, *Senior Member, IEEE*

***Abstract*—In this paper, adaptive variable structure neural control is investigated for a class of nonlinear systems under the effects of time-varying state delays and uncertain hysteresis inputs. The unknown time-varying delay uncertainties are compensated for using appropriate Lyapunov–Krasovskii functionals in the design, and the effect of the uncertain hysteresis with the Prandtl–Ishlinskii (PI) model representation is also mitigated using the proposed control. By utilizing the integral-type Lyapunov function, the closed-loop control system is proved to be semiglobally uniformly ultimately bounded (SGUUB). Extensive simulation results demonstrate the effectiveness of the proposed approach.**

***Index Terms*—Neural networks (NNs), Prandtl–Ishlinskii (PI) hysteresis model, time-varying delays, variable structure control.**

I. Introduction

In recent years, control of nonlinear systems preceded by unknown hysteresis nonlinearities has received a great deal of attention, since hysteresis nonlinearities are common in many industrial processes, especially in position control of smart material-based actuators, including piezoceramics and shape memory alloys. Control of a system with hysteresis nonlinearities is challenging, because they are nondifferentiable nonlinearities and severely limit system performance by giving rise to undesirable inaccuracy or oscillations, and even lead to closed-loop instability [1]. Furthermore, due to the nonsmooth characteristics of hysteresis nonlinearities, traditional control methods are inadequate in dealing with the effects of unknown hysteresis. Therefore, advanced control techniques to mitigate the effects of hysteresis have been called upon and have been studied for decades.

In [1], adaptive control with an adaptive hysteresis inverse was presented for plants with unknown parameterized hysteresis. Robust control was developed by combining the inverse compensation for a novel dynamic hysteresis model in magnetostrictive actuators in [2]. In [3], robust adaptive control was investigated for a class of nonlinear system with unknown backlash-like hysteresis, for which, adaptive backstepping control was designed in [4]. Apart from the above hysteresis models, there exist many other hysteresis models in the literature, since hysteresis is a very complex phenomenon. Interested readers can refer to [5] for a review of the hysteresis models. For different kinds of hysteresis models, different compensation methods should be adopted. As such, it is challenging to fuse those hysteresis models with the available control techniques. It appears that the Prandtl–Ishlinskii (PI) hysteresis model, which is a subclass of Preisach-type model, can be explored in connection with the existing robust adaptive control methods. In [6] and [7], adaptive variable structure control and adaptive backstepping methods were proposed, respectively, for a class of continuous-time nonlinear dynamic systems preceded by hysteresis nonlinearity with the PI hysteresis model representation. However, since the nonlinear functions in most of the above works were assumed to be known, it is therefore of interest to develop methods to deal with unknown nonlinearities, so as to enlarge the class of applicable systems.

Other than hysteresis, time delay is another problem that is often encountered in physical systems, for example, in the turbojet engines, aircraft systems, microwave oscillators, nuclear reactors, rolling mills, chemical processes, and hydraulic systems, among others [8]. The existence of time delays in a system frequently becomes a source of instability, and may degrade the control performance. The control of the time-delay systems is challenging since they involve infinite-dimensional functional differential equations, which are more difficult to handle than finite-dimensional ordinary differential equations [9]. To guarantee the stability of time-delay systems, a number of different approaches have been proposed [10]. Lyapunov–Krasovskii functionals [11], combined with the linear matrix inequality (LMI) technique, have been used to establish a framework for the stability and control of time-delay systems [12]–[15]. In [16], Lyapunov–Krasovskii functionals were used with backstepping for a class of single-input–single-output (SISO) nonlinear time-delay systems with a "triangular structure," which was later commented that it could not be "constructively obtained" in [17]. The need for knowledge of system nonlinearities was removed with the use of adaptive neural network (NN) control in [18], which was extended to a class of multiple-input–multiple-output (MIMO) nonlinear systems in block-triangular form with unknown state

Manuscript received June 11, 2008; revised December 03, 2008; accepted February 07, 2009. First published May 27, 2009; current version published July 09, 2009. This work was supported in part by A*STAR SERC Singapore under Grant 052 101 0097.

B. Ren, S. S. Ge, and T. H. Lee are with the Department of Electrical and Computer Engineering, National University of Singapore, Singapore 117576, Singapore (e-mail: renbeibei@nus.edu.sg; samge@nus.edu.sg; eleleeth@nus.edu.sg).

C.-Y. Su is with the Department of Mechanical and Industrial Engineering, Concordia University, Montreal, QC H3G 1M8 Canada (e-mail: cysu@alcor.concordia.ca).

Color versions of one or more of the figures in this paper are available online at http://ieeexplore.ieee.org.

Digital Object Identifier 10.1109/TNN.2009.2016959

delays [19]. Apart from the Lyapunov–Krasovskii method, the Lyapunov–Razumikhin technique has also been investigated for linear time-delay systems [20], as well as for nonlinear time-delay systems [21], [22].

Although there are some works that deal with hysteresis, or time delay, individually, the combined problem, despite its practical relevance, is largely open in the literature to the best of our knowledge, with the exception of [23], in which turning cutting systems were modeled as plants containing linearly parameterized nonlinearities, backlash hysteresis, and known constant time delay. Motivated by [23], in this paper, we make several technical contributions as follows.

First, we remove the restriction of linearly parameterized nonlinear systems considered in [23], and tackle a larger and more complex class of nonlinear systems with unknown nonlinearities, for which direct approximation-based control using NNs is adopted due to their universal approximation capabilities.

Second, we consider nonlinear systems that are preceded by uncertain hysteresis inputs in the PI form, which is more complex than the backlash type, but can capture the hysteresis phenomenon more accurately. We fuse the PI hysteresis with adaptive neural control to the reduce the effects of uncertain hysteresis.

Third, we relax the assumption of known constant time delay considered in [23], to unknown time-varying delay in our paper, for which Lyapunov–Krasovskii functionals are used to compensate.

The organization of this paper is as follows. The problem formulation and preliminaries are given in Section II. In Section III, adaptive variable structure neural control is developed for a class of single-input–single-output (SISO) time-varying state delay systems with hysteresis by utilizing an integral-type Lyapunov function first, which is extended to MIMO systems later. Results of extensive simulation studies are shown to demonstrate the effectiveness of the approach in Section IV, followed by conclusion in Section V.

II. Problem Formulation and Preliminaries

A. Prandtl–Ishlinskii Hysteresis Model

First, we briefly introduce the PI hysteresis model which is adopted in this paper. According to [6] and [7], the PI hysteresis model with a play operator can be represented as follows:

$$u_i(t) = p_{i0}v_i(t) - d_i[v_i](t) \tag{1}$$

$$p_{i0} = \int_0^R p_i(r)dr$$

$$d_i[v_i](t) = \int_0^R p_i(r)F_{ir}[v_i](t)dr$$

$$F_{ir}[v_i](0) = f_{ir}\left(v_i(0), 0\right)$$

$$F_{ir}[v_i](t) = f_{ir}\left(v_i(t), F_{ir}[v_i](t_k)\right), \quad \text{for } t_k < t \leq t_{k+1} \text{ and } 0 \leq k \leq N-1$$

$$f_{ir}(v, w) = \max\left(v - r, \min(v + r, w)\right) \tag{2}$$

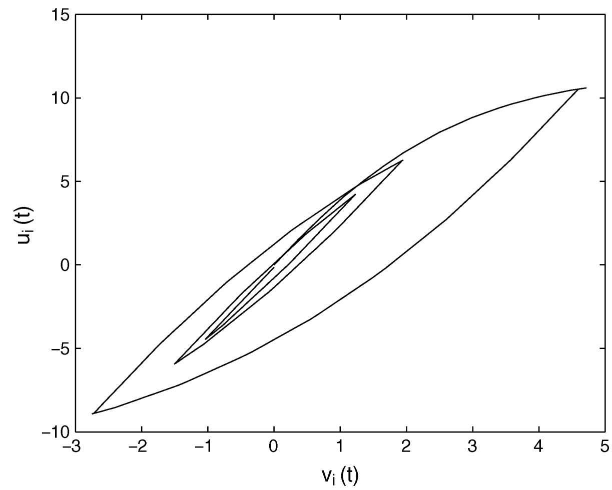

Fig. 1. Hysteresis curves given by $u_i(t) = p_{i0}v_i(t) - d_i[v_i](t)$.

where $u_i(t) \in R$ and $v_i(t) \in R$ are the output and the input of PI hysteresis model, respectively; $p_i(r)$ is a given density function, satisfying $p_i(r) \geq 0$ with $\int_0^\infty rp_i(r)dr < \infty$; and F_{ir} is known as the play operator. In addition, there are N subintervals, and the function v_i is monotone on each of the subintervals $(t_k, t_{k+1}]$. The density function $p_i(r)$ vanishes for large values of r. As such, it is reasonable to choose a large enough constant R such that the given density function $p_i(R)$ vanishes, despite the fact that $R = \infty$ is commonly chosen as the upper limit of integration in the literature. For the detailed description about the PI hysteresis model, the interested readers can refer to [6], [7], and references therein. As an illustration, Fig. 1 shows $u_i(t)$ generated by (1), with $p_i(r) = e^{-0.067(r-1)^2}$, $r \in [0, 10]$, and the input $v_i(t) = 7\sin(3t)/(1+t)$, $t \in [0, 2\pi]$. This numerical result shows that the PI hysteresis model (1) indeed generates hysteresis curves.

B. Problem Formulation

Consider the following class of uncertain MIMO nonlinear system Σ_0 consisting of interconnected subsystems in a Brunovsky form with time-varying state delays and uncertain PI hysteresis inputs:

$$\Sigma_0 : \begin{cases} \dot{x}_{i,j} = x_{i,j+1} \\ \dot{x}_{i,n_i} = f_i(x, \bar{u}_{i-1}) + g_{i,\tau}(x_\tau) + b_i(\bar{x}_i)u_i \\ x_i(t) = \psi_i(t), \qquad t \in [-\tau_{\max}, 0] \\ y_i = x_{i,1} \end{cases} \tag{3}$$

where $i = 1, 2, \ldots, m$, $j = 1, 2, \ldots, n_i - 1$; $x_i = [x_{i,1}, \ldots, x_{i,n_i}]^T \in R^{n_i}$ are the delay-free state variables of the ith subsystem, $\bar{x}_i = [x_1^T, \ldots, x_i^T]^T \in R^{\bar{n}_i}$ with $\bar{n}_i = \sum_{j=1}^i n_j$ and $x = [x_1^T, x_2^T, \ldots, x_m^T]^T \in R^n$ with $n = \sum_{i=1}^m n_i$; $y_i \in R$ denotes the ith subsystem output; $f_i(\cdot)$ and $g_{i,\tau}(\cdot)$ are unknown continuous functions; $b_i(\cdot)$ are the unknown differentiable control gains; $\psi_i(t)$ are the smooth and bounded initial functions; $x_\tau = [x_1(t-\tau_1(t))^T, \ldots, x_m(t-\tau_m(t))^T]^T$, and $\tau_1(t), \ldots, \tau_m(t)$ are unknown time-varying state delays, $\tau_{\max}$ as will be defined later is a known positive constant; $\bar{u}_i = [u_1, u_2, \ldots, u_i]^T$, and $u_i \in R$ is the input of the ith subsystem and the output of the ith hysteresis.

Substituting the PI hysteresis model (1) into the plant (3), we obtain the integrated system Σ_1

$$\Sigma_1 : \begin{cases} \dot{x}_{i,j} = x_{i,j+1} \\ \dot{x}_{i,n_i} = f_i(x, \bar{u}_{i-1}) + g_{i,\tau}(x_\tau) + b_i(\bar{x}_i) p_{i0} v_i(t) \\ \quad -b_i(\bar{x}_i) d_i[v_i](t) \\ x_i(t) = \psi_i(t), \qquad t \in [-\tau_{\max}, 0] \\ y_i = x_{i,1}. \end{cases} \tag{4}$$

Our control objective is to track the specified desired trajectory y_{id} to a small neighborhood of zero with the output y_i, while ensuring that all the signals in the corresponding closed-loop system are semiglobally uniformly ultimately bounded (SGUUB).

Remark 1: Although it appears possible to rewrite (4) into the nonaffine form $\dot{x} = f(x, u)$, it still cannot be handled by the method proposed by [24], in which implicit function theorem was adopted to handle the nonaffine problem. The reason is that if we want to apply implicit function theorem to a function, one requirement is that the first-order derivative of the function is not equal to zero. However, due to the nonsmooth characteristics of hysteresis, the function $f(x, u)$ transformed from (4) is nondifferentiable and thus does not satisfy the conditions of applying implicit function theorem. Therefore, we need to seek for new solutions in this paper.

Remark 2: Noticing that $d_i[v_i](t)$ in (4) is an integral function of control input signal v_i, which needs to be designed later, we cannot assume $d_i[v_i](t)$ is bounded before we prove the boundedness of control input v_i, even if the output of PI model is bounded for bounded input. Therefore, standard robust adaptive control used for dealing with bounded disturbance cannot be applied here. To solve this problem, we will develop the comprehensive control in the subsequent Section III.

Assumption 1: There exist two positive constants b_{i0} and b_{i1}, such that $0 < b_{i0} \le |b_i(\bar{x}_i)| \le b_{i1}, \forall \bar{x}_i \in R^{\bar{n}_i}$.

Remark 3: Assumption 1 implies that smooth functions $b_i(\bar{x}_i)$ are either strictly positive or strictly negative, which is reasonable because $b_i(\bar{x}_i)$ being bounded away from zero is the controllable condition of system Σ_1 in (4), which is necessary in most control schemes [25], [26]. Without loss of generality, we will assume that $b_i(\bar{x}_i) > 0$, $\forall \bar{x}_i \in R^{\bar{n}_i}$. In addition, the constants b_{i0} and b_{i1} need not be known, as they are used in the stability analysis only.

Assumption 2: The desired trajectory y_{id} and its time derivatives up to the n_ith-order remain bounded, i.e., $\bar{x}_{id} = [y_{id}, \dot{y}_{id}, \ddot{y}_{id}, \ldots y_{id}^{(n_i)}]^T \in \Omega_{id} \subset R^{n_i+1}$ with known compact set $\Omega_{id}, i = 1, \ldots, m$.

Assumption 3: The unknown time-varying state delays $\tau_i(t)$ satisfy the following inequalities:

$$0 \le \tau_i(t) \le \tau_{\max},\ \dot{\tau}_i(t) \le \bar{\tau}_{\max} < 1, \qquad i = 1, \ldots, m \tag{5}$$

with known constants $\tau_{\max}$ and $\bar{\tau}_{\max}$.

Assumption 4: There exist known constants $p_{i0\min}$ and $p_{i\max}$, such that $p_{i0} > p_{i0\min}$, and $p_i(r) \le p_{i\max}$ for all $r \in [0, R]$, $i = 1, \ldots m$.

Remark 4: It is reasonable to set an upper bound for the density function $p_i(r)$, based on its properties that $p_i(r) \ge 0$ with $\int_0^R r p_i(r) dr < \infty$.

C. RBFNN Approximation

In control engineering, radial basis function neural network (RBFNN) has been successfully used as a linearly parameterized function approximator to achieve various objectives, such as modeling, identification, and feedback linearization, by virtue of its the universal approximation capabilities, learning and adaptation, and parallel distributed structures [27], [28]. In this paper, the following RBFNN [29] is used to approximate the continuous function $h(Z) : R^q \to R$:

$$h_{\text{nn}}(Z, W) = W^T S(Z) \tag{6}$$

where the input vector $Z \in \Omega \subset R^q$, weight vector $W = [w_1, w_2, \ldots, w_l]^T \in R^l$, with the NN node number $l > 1$; and $S(Z) = [s_1(Z), \ldots, s_l(Z)]^T$, with $s_i(Z)$ being chosen as the commonly used Gaussian functions, which have the form

$$s_i(Z) = \exp\left[\frac{-(Z - \mu_i)^T (Z - \mu_i)}{\eta^2}\right], \qquad i = 1, 2, \ldots, l \tag{7}$$

where $\mu_i = [\mu_{i1}, \mu_{i2}, \ldots, \mu_{iq}]^T$ is the center of the receptive field and η is the width of the Gaussian function.

It has been proven that network (6) can approximate any continuous function over a compact set $\Omega_Z \subset R^q$ to any arbitrary accuracy as

$$h(Z) = h_{\text{nn}}(Z, W^*) + \varepsilon(Z) \qquad \forall Z \in \Omega_Z \tag{8}$$

where W^* is ideal NN weights, and $\varepsilon(Z)$ is the NN approximation error.

Assumption 5: There exist ideal constant weights W^* such that $|\varepsilon(Z)| \le \varepsilon^*$ with constant $\varepsilon^* > 0$ for all $Z \in \Omega_Z$. Moreover, W^* is bounded by $\|W^*\| \le w_m$ on the compact set Ω_Z.

The ideal weights W^* are "artificial" quantities that are required for analytical purposes. According to the discussion in [30], W^* is defined as follows:

$$W^* = \arg\min_{(W)} \left[\sup_{Z \in \Omega_Z} |h_{\text{nn}}(Z, W) - h(Z)|\right]$$

which is unknown and needs to be estimated in control design. Let $\hat{W}$ be the estimate of W^* and the weight estimation error be $\tilde{W} = \hat{W} - W^*$.

Remark 5: Although RBFNN is employed in our control design, it can be replaced by other linearly parameterized function approximators such as high-order NNs, fuzzy systems, polynomials, splines and wavelet networks without difficulty. For a unified framework of different approximation structures in adaptive approximation-based control, interested readers can refer to [31].

D. Preliminaries

The following lemma will be used for control design and system stability analysis in the remainder of this paper.

Lemma 1 [32]: For any continuous function $h(\xi_1, \ldots, \xi_n) : R^{m_1} \times \ldots \times R^{m_n} \to R$ satisfying $h(0, \ldots, 0) = 0$, where $\xi_j \in R^{m_j} (j = 1, 2, \ldots, n, m_j > 0)$, there exist positive smooth functions $\varrho_j(\xi_j) : R^{m_j} \to R (j = 1, 2, \ldots, n)$ satisfying $\varrho_j(0) = 0$ such that

$$h(\xi_1, \ldots, \xi_n) \le \sum_{j=1}^{n} \varrho_j(\xi_j). \tag{9}$$

Remark 6: According to Lemma 1, the unknown continuous functions of delayed states in (4), $g_{i,\tau}(x_\tau)$, satisfy the inequality

$$g_{i,\tau}(x_\tau) \le \sum_{k=1}^{m} \varrho_{ik}\left(x_k\left(t - \tau_k(t)\right)\right) \tag{10}$$

with $\varrho_{ik}(\cdot)$ being positive continuous functions, $i = 1, \ldots, m$. In this paper, we consider the special case whereby the bounding functions $\varrho_{ik}(\cdot)$ are known. As for the case of unknown bounding functions, interested readers can refer to [19].

Throughout this paper, $\tilde{(\cdot)} = \hat{(\cdot)} - (\cdot)$, $\|\cdot\|$ denotes the 2-norm, and $\lambda_{\min}(\cdot)$ and $\lambda_{\max}(\cdot)$ denote the smallest and largest eigenvalues of a square matrix $(\cdot)$, respectively. The following function $q(x|c)$, with a positive constant c, is introduced for the purpose of the control design:

$$q(x|c) = \begin{cases} 1, & \text{if } |x| \ge c \\ 0, & \text{if } |x| < c \end{cases} \qquad \forall x \in R. \tag{11}$$

III. Control Design and Stability Analysis

In this section, we will carry out adaptive NN control design for system Σ_1 in (4) to achieve stable output tracking. In order to illustrate the design methodology clearly, the SISO case (i.e., $m = 1$) is discussed first, which is generalized to the MIMO case (i.e., $m \ge 2$) subsequently. For both cases, the closed-loop system will be proved to be SGUUB by Lyapunov stability analysis.

The following definitions and notations are used throughout the control design and stability analysis. Define x_{id} and e_i as

$$x_{id} = \left[y_{id}, \dot{y}_{id}, \ldots, y_{id}^{(n_i-1)}\right]^T$$
$$e_i = x_i - x_{id} = \left[e_{i1}, e_{i2}, \ldots, e_{in_i}\right]^T$$

and the filtered tracking error s_i as

$$s_i = \left(\frac{d}{dt} + \lambda_i\right)^{n_i-1} e_{i1} = \sum_{j=1}^{n_i-1} \lambda_{ij} e_{ij} + e_{in_i} \tag{12}$$

where λ_{ij} are chosen such that the polynomial $\sum_{j=1}^{n_i-1} \lambda_{ij} e_{ij} + e_{in_i}$ is a Hurwitz polynomial.

A. Adaptive NN Control for SISO Case $(m = 1)$

For the SISO case where $m = 1$, system (4) can be rewritten in the following form:

$$\Sigma_{11} : \begin{cases} \dot{x}_{1,j} = x_{1,j+1}, \qquad j = 1, 2, \ldots, n_1 - 1 \\ \dot{x}_{1,n_1} = f_1(x_1) + g_{1,\tau}\left(x_1\left(t - \tau_1(t)\right)\right) \\ \quad + b_1(x_1) p_{10} v_1(t) - b_1(x_1) d_1[v_1](t) \\ x_1(t) = \psi_1(t), \qquad t \in [-\tau_{\max}, 0] \\ y_1 = x_{1,1}. \end{cases} \tag{13}$$

Substituting (13) into (12) leads to

$$\dot{s}_1 = f_1(x_1) + g_{1,\tau}\left(x_1\left(t - \tau_1(t)\right)\right) + b_1(x_1) p_{10} v_1 - b_1(x_1) d_1[v_1](t) + \nu_1 \tag{14}$$

where $\nu_1 = \sum_{j=1}^{n_1-1} \lambda_{1j} e_{1,j+1} - y_{1d}^{(n_1)}$.

Define the following integral Lyapunov function candidate, which was first proposed in [33] to avoid control singularity:

$$V_{s1} = \int_0^{s_1} \frac{\sigma}{b_1\left(\bar{x}_1^+, \sigma + \beta_1\right)} d\sigma \tag{15}$$

where $\beta_1 = y_{1d}^{(n_1-1)} - \sum_{j=1}^{n_1-1} \lambda_{1j} e_{1j}$, and $\bar{x}_1^+ = [x_{1,1}, \ldots, x_{1,n_1-1}]^T$. Then, V_{s1} can be rewritten as the following form by using the first mean value theorem for integrals:

$$V_{s1} = \frac{\lambda_{s1} s_1^2}{b_1\left(\bar{x}_1^+, \lambda_{s1} s_1 + \beta_1\right)}, \qquad \lambda_{s1} \in (0, 1).$$

According to Assumption 1, $0 < b_{10} \le b_1(x_1)$, it is clear that V_{s1} is positive definite with respect to s_1. Differentiating V_{s1} with respect to time t, we obtain

$$\begin{aligned} \dot{V}_{s1} &= \frac{\partial V_{s1}}{\partial s_1} \dot{s}_1 + \frac{\partial V_{s1}}{\partial \bar{x}_1^+} \dot{\bar{x}}_1^+ + \frac{\partial V_{s1}}{\partial \beta_1} \dot{\beta}_1 \\ &= \frac{s_1}{b_1(x_1)} \dot{s}_1 + \int_0^{s_1} \sigma \left[\frac{\partial b_1^{-1}\left(\bar{x}_1^+, \sigma + \beta_1\right)}{\partial \bar{x}_1^+} \dot{\bar{x}}_1^+\right] d\sigma \\ &\quad + \dot{\beta}_1 \int_0^{s_1} \sigma \left[\frac{\partial b_1^{-1}\left(\bar{x}_1^+, \sigma + \beta_1\right)}{\partial \beta_1}\right] d\sigma. \end{aligned} \tag{16}$$

Due to $\partial b_1^{-1}(\bar{x}_1^+, \sigma + \beta_1)/\partial \beta_1 = \partial b_1^{-1}(\bar{x}_1^+, \sigma + \beta_1)/\partial \sigma$ and $\dot{\beta}_1 = -\nu_1$, it is shown that

$$\dot{\beta}_1 \int_0^{s_1} \sigma \left[\frac{\partial b_1^{-1}\left(\bar{x}_1^+, \sigma + \beta_1\right)}{\partial \beta_1}\right] d\sigma = -\frac{\nu_1 s_1}{b_1(x_1)} + \int_0^{s_1} \frac{\nu_1}{b_1\left(\bar{x}_1^+, \sigma + \beta_1\right)} d\sigma. \tag{17}$$

Substituting (14) and (17) into (16) results in

$$\begin{aligned} \dot{V}_{s1} &= \frac{s_1}{b_1(x_1)} \left[f_1(x_1) + g_{1,\tau}\left(x_1\left(t - \tau_1(t)\right)\right) + b_1(x_1) p_{10} v_1 - b_1(x_1) d_1[v_1](t) + \nu_1\right] \\ &\quad + \int_0^{s_1} \sigma \left[\sum_{k=1}^{n_1-1} \frac{\partial b_1^{-1}\left(\bar{x}_1^+, \sigma + \beta_1\right)}{\partial x_{1k}} x_{1,k+1}\right] d\sigma \\ &\quad - \frac{\nu_1 s_1}{b_1(x_1)} + \int_0^{s_1} \frac{\nu_1}{b_1\left(\bar{x}_1^+, \sigma + \beta_1\right)} d\sigma. \end{aligned} \tag{18}$$

Using (10) and Young's inequality, (18) becomes

$$\dot{V}_{s1} \le s_1 Q_1(Z_1) + s_1\left[p_{10} v_1 - d_1[v_1](t)\right] + \frac{1}{2} \varrho_{11}^2\left(x_1\left(t - \tau_1(t)\right)\right) + \frac{s_1^2}{2 b_1^2(x_1)} \tag{19}$$

where

$$Q_1(Z_1)=\frac{f_1(x_1)}{b_1(x_1)}+\frac{1}{s_1}\int_0^{s_1}\left[\sigma\sum_{k=1}^{n_1-1}\frac{\partial b_1^{-1}\left(\bar{x}_1^+,\sigma+\beta_1\right)}{\partial x_{1k}}x_{1,k+1}+\frac{\nu_1}{b_1\left(\bar{x}_1^+,\sigma+\beta_1\right)}\right]d\sigma$$
$$=\frac{f_1(x_1)}{b_1(x_1)}+\int_0^1\left[\theta s_1\sum_{k=1}^{n_1-1}\frac{\partial b_1^{-1}\left(\bar{x}_1^+,\theta s_1+\beta_1\right)}{\partial x_{1k}}x_{1,k+1}+\frac{\nu_1}{b_1\left(\bar{x}_1^+,\theta s_1+\beta_1\right)}\right]d\theta$$

with $Z_1=[x_1^T,s_1,\nu_1,\beta_1]^T\in R^{n_1+3}$.

To overcome the design difficulties from the unknown time-varying delays $\tau_1(t)$ in (19), the following Lyapunov–Krasovskii functional can be considered [34]:

$$V_{U_1}(t)=\frac{1}{2(1-\bar{\tau}_{\max})}\int_{t-\tau_1(t)}^{t}\varrho_{11}^2\left(x_1(\tau)\right)d\tau. \quad (20)$$

The time derivative of V_{U_1} can be expressed as follows:

$$\dot{V}_{U_1}(t)=\frac{1}{2(1-\bar{\tau}_{\max})}\times\left[\varrho_{11}^2\left(x_1(t)\right)-\varrho_{11}^2\left(x_1\left(t-\tau_1(t)\right)\right)\left(1-\dot{\tau}_1(t)\right)\right] \quad (21)$$

which can be used to cancel the time delay term on the right-hand side of (19), thus circumvent the design difficulty due to the unknown time-varying delay $\tau_1(t)$, without introducing any additional uncertainties to the system. For concise notation, the time variables t and $t-\tau_1(t)$ will be omitted whenever the time-varying delay term is eliminated, in the remainder of this paper.

Combining (19) and (21), we obtain

$$\dot{V}_{s1}+\dot{V}_{U1}\leq s_1h_1(Z_1)+s_1\left[p_{10}v_1-d_1[v_1](t)\right] \quad (22)$$

where

$$h_1(Z_1)=Q_1(Z_1)+\frac{s_1}{2b_1^2(x_1)}+\frac{1}{2(1-\bar{\tau}_{\max})s_1}\varrho_{11}^2(x_1). \quad (23)$$

Remark 7: Note that $h_1(Z_1)$ in (23) contains the term $(1/2(1-\bar{\tau}_{\max})s_1)\varrho_{11}^2(x_1)$, which is not well defined at $s_1=0$ and may lead to the controller singularity problem, if we utilize $h_1(Z_1)$ to construct the control law. As such, care must be taken to guarantee the boundedness of the control as discussed in [34]. It is noted that the controller singularity takes place at the point $s_1=0$, where the control objective is supposed to be achieved. From a practical point of view, once the system reaches its origin, no control action should be taken for less power consumption. As $s_1=0$ is hard to detect owing to the existence of measurement noise, it is more practical to relax our control objective of convergence to a "ball" rather than the origin.

Define the following compact sets:

$$\Omega_{Z_1}=\left\{\left[x_1^T,s_1,\nu_1,\beta_1\right]^T|x_1\in\Omega_1,x_{1d}\in\Omega_{1d}\right\} \quad (24)$$
$$\Omega_{c_{s_1}}=\{s_1||s_1|<c_{s_1},x_{1d}\in\Omega_{1d}\} \quad (25)$$
$$\Omega_{Z_1}^0=\Omega_{Z_1}-\Omega_{c_{s_1}} \quad (26)$$

where $\Omega_1\subset R^{n_1}$ is a sufficiently large compact set satisfying $\Omega_1\supset\Omega_{10}$ defined later in Theorem 1, and c_{s_1} is a positive design constant that can be chosen arbitrarily small and "−" in (26) is used to denote the complement set of set $\Omega_{c_{s_1}}$. In addition, it has been shown that $\Omega_{Z_1}^0$ is a compact set in [34].

Let $\hat{W}_1^TS(Z_1)$ be the approximation of the function $h_1(Z_1)$, defined in (23), on the compact set $\Omega_{Z_1}^0$. Then, using RBFNN as discussed in Section II-C, we have

$$h_1(Z_1)=\hat{W}_1^TS(Z_1)-\tilde{W}_1^TS(Z_1)+\varepsilon_1(Z_1) \quad (27)$$

where the approximation error $\varepsilon_1(Z_1)$ satisfies $|\varepsilon_1(Z_1)|\leq\varepsilon_1^*$ with positive constant ε_1^*, $\forall Z_1\in\Omega_{Z_1}^0$.

For (22), we design a control law as follows:

$$v_1=-q\left(s_1|c_{s_1}\right)\frac{\mathrm{sgn}(s_1)}{p_{10\min}}\left[k_{10}(t)|s_1|+\left|\hat{W}_1^TS(Z_1)\right|\right]+v_{1h} \quad (28)$$
$$v_{1h}=-q\left(s_1|c_{s_1}\right)\frac{\mathrm{sgn}(s_1)}{p_{10\min}}\int_0^R\hat{p}_1(t,r)\left|F_{1r}[v_1](t)\right|dr \quad (29)$$
$$k_{10}(t)=q\left(s_1|c_{s_1}\right)\left(k_{11}+k_{12}(t)+\frac{1}{2}\right) \quad (30)$$

where $q(s_1|c_{s_1})$ is defined in (11), $\hat{p}_1(t,r)$ is the estimate of the density function $p_1(r)$, k_{11} is a positive constant, and $k_{12}(t)$ is chosen as

$$k_{12}(t)=q\left(s_1|c_{s_1}\right)\frac{k_{13}}{2(1-\bar{\tau}_{\max})s_1^2}\int_{t-\tau_{\max}}^{t}\varrho_{11}^2\left(x_1(\tau)\right)d\tau \quad (31)$$

with k_{13} as a positive constant specified by the designer.

The adaptation laws are designed as follows:

$$\dot{\hat{W}}_1=q\left(s_1|c_{s_1}\right)\Gamma_1\left[S(Z_1)s_1-\sigma_{w_1}\hat{W}_1\right] \quad (32)$$
$$\frac{\partial}{\partial t}\hat{p}_1(t,r)=\begin{cases}-q\left(s_1|c_{s_1}\right)\eta_1\sigma_{p_1}\hat{p}_1(t,r), & \text{if } \hat{p}_1(t,r)\geq p_{1\max}\\ q\left(s_1|c_{s_1}\right)\eta_1\left[|s_1||F_{1r}\left[x_{1,n_1}\right](t)|-\sigma_{p_1}\hat{p}_1(t,r)\right], & \text{if } 0\leq\hat{p}_1(t,r)<p_{1\max}\end{cases} \quad (33)$$

with $\Gamma_1>0$, σ_{w_1}, σ_{p_1}, and η_1 being strictly positive constants.

Remark 8: The term v_{1h} in (29) is used to cancel the effect caused by the hysteresis term $d_1[v_1](t)$. Unlike traditional robust adaptive controller designs, where $d_1[v_1](t)$ is either assumed to be bounded by a constant or a known function, $d_1[v_1](t)$ here is presented as an integral function of control input signal v_1, and there are no assumptions on its boundedness. Considering that the density function $p_1(r)$ is not a function of time, it can be treated as a "parameter" of the hysteresis model and adaption law can be developed to obtain an estimate of it. This is crucial for the success of the adaption law design [6].

Remark 9: From (28) and (29), we notice that both sides of (28) contain the control signal v_1, because v_{1h} depends on v_1 as can be seen from (29). This is known as the fixed-point problem, where the solvability of v_1 can be proved following the proof of Theorem 1.4 about the existence of the hysteresis inverse operator in [35]. Since it is difficult to obtain the explicit solution for v_1 from (28), we introduce several possible implementation methods instead of solving v_1 directly from (28). One is the time-scale separation approach, recently proposed in [36]: the control signal $v_1(t)$ is a solution of a "fast" dynamical equation, which means the dynamics of the controller is faster than that of the system plant. Thus, time-scale separation is achieved between the system plant and the controller dynamics using the singular perturbation theory. Second method is adopting the numerical implementation of the inverse hysteresis operator as in [35], where a real-time inverse feedforward control was designed for piezoelectric actuators. In this paper, we introduce a small delay to evaluate the input: at time t, we use $v_1(t-\triangle t)$ to compute v_{1h} in (29) for suitably small Δt, such that $v_1(t)$ in (28) becomes a function of $s_1, \hat{W}_1, \hat{p}_1(t,r), v_1(t-\triangle t)$. The limitation of this method is that its accuracy depends on the choice of Δt. The effects of the variations of Δt will be investigated later in the simulation part in Section IV.

Theorem 1: Consider the closed-loop system consisting of the plant (13), the control laws (28) and (29), and adaptation laws (32) and (33). Under Assumptions 1–4, given some initial conditions $x_1(0)$, $\hat{W}_1(0)$, belong to Ω_{10}, we can conclude that the overall closed-loop neural control system is SGUUB in the sense that all of the signals in the closed-loop system are bounded, i.e., the states and the weights in the closed-loop system will remain in the compact set Ω_1 defined by

$$\Omega_1=\left\{s_1,\tilde{W}_1 \middle| |s_1| \le \sqrt{2\mu_1}, \|\tilde{W}_1\|\le\sqrt{\frac{2\mu_1}{\lambda_{\min}\left(\Gamma_1^{-1}\right)}}\right\} \quad (34)$$

with

$$\begin{aligned}\mu_1 &= \frac{\mu_{11}}{\lambda_{11}} + V_1(0)\\ \mu_{11} &= \frac{\sigma_{p_1}R}{2}p_{1\max}^2 + \frac{\sigma_{w_1}}{2}\|W_1^*\|^2 + \frac{\varepsilon_1^{*2}}{2}\\ \lambda_{11} &= \min\left\{\frac{b_{10}k_{11}}{\lambda_{s1}}, k_{13}, \frac{\sigma_{w_1}}{\lambda_{\max}\left(\Gamma_1^{-1}\right)}, \sigma_{p_1}\eta_1\right\}\end{aligned} \quad (35)$$

$$V_1(0) = V_{s1}(0) + V_{U_1}(0) + \frac{1}{2}\tilde{W}_1^T(0)\Gamma_1^{-1}\tilde{W}_1(0) + \frac{1}{2\eta_1}\int_0^R \tilde{p}_1^2(0,r)dr \quad (36)$$

and the tracking error will converge to a neighborhood of zero. In addition, the states and the weights in the closed-loop system will eventually converge to the compact set Ω_{1s} defined by

$$\Omega_{1s}=\left\{s_1,\tilde{W}_1 \middle| |s_1| \le \sqrt{2\mu_1^*}, \|\tilde{W}_1\|\le\sqrt{\frac{2\mu_1^*}{\lambda_{\min}\left(\Gamma_1^{-1}\right)}}\right\} \quad (37)$$

where $\mu_1^* = \mu_{11}/\lambda_{11}$.

Proof: The method of proof is generally similar to that in our previous works [37], [38], although the details of analysis are different and more complex, due to the presence of time delay and hysteresis in the system. In this proof, we will show that for a compact set $\Omega_{\rm NN}$, on which the NN approximation is valid, there exist some control parameters and a nonempty initial compact set Ω_{10}, such that as long as the initial conditions start in Ω_{10}, the states and the weights will remain in the conservative compact set Ω_1, and finally converge to the compact set Ω_{1s}. Both of them belong to the chosen compact set $\Omega_{\rm NN}$. The proof includes two steps, and one could see the whole picture at the end of the proof of Step 2.

Step 1: Suppose that both the states and the weights belong to $\Omega_{\rm NN}$, i.e., $\{x_1, \hat{W}_1\} \in \Omega_{\rm NN}$, $\forall t \ge 0$, on which NN approximation (27) is valid.

Consider the following Lyapunov function candidate:

$$V_1(t) = V_{s1}(t) + V_{U_1}(t) + \frac{1}{2}\tilde{W}_1^T\Gamma_1^{-1}\tilde{W}_1 + \frac{1}{2\eta_1}\int_0^R \tilde{p}_1^2(t,r)dr \quad (38)$$

where $\tilde{W}_1 = \hat{W}_1 - W_1$ and $\tilde{p}_1(t,r) = \hat{p}_1(t,r) - p(r)$. Differentiating $V_1(t)$ with respect to time t

$$\dot{V}_1(t) = \dot{V}_{s1}(t) + \dot{V}_{U_1}(t) + \tilde{W}_1^T\Gamma_1^{-1}\dot{\hat{W}}_1 + \frac{1}{\eta_1}\int_0^R \tilde{p}_1(t,r)\frac{\partial}{\partial t}\hat{p}_1(t,r)dr. \quad (39)$$

Substituting (22) into (39) leads to

$$\dot{V}_1(t) \le s_1h_1(Z_1) + s_1\left[p_{10}v_1 - d_1[v_1](t)\right] + \tilde{W}_1^T\Gamma_1^{-1}\dot{\hat{W}}_1 + \frac{1}{\eta_1}\int_0^R \tilde{p}_1(t,r)\frac{\partial}{\partial t}\hat{p}_1(t,r)dr. \quad (40)$$

Considering the adaptive neural control laws and adaptation laws from (28)–(33), the stability analysis is carried out in the following two regions, respectively.

- **Region 1**: If $|s_1| \ge c_{s_1}$, then $q_1(s_1|c_{s_1}) = 1$. Noting (27) and submitting (28) into (40), we have

$$\begin{aligned}\dot{V}_1(t) \le& - s_1\tilde{W}_1^TS(Z_1) + s_1\varepsilon_1(Z_1) - k_{10}(t)s_1^2\\ &+ s_1\left[p_{10}v_{1h} - d_1[v_1](t)\right] + \tilde{W}_1^T\Gamma_1^{-1}\dot{\hat{W}}_1\\ &+ \frac{1}{\eta_1}\int_0^R \tilde{p}_1(t,r)\frac{\partial}{\partial t}\hat{p}_1(t,r)dr.\end{aligned} \quad (41)$$

  Using Young's inequality, we have

$$s_1\varepsilon_1(Z_1) \le \frac{s_1^2}{2} + \frac{\varepsilon_1^{*2}}{2}. \quad (42)$$

  Substituting (30), (32), and (42) into (41) leads to

$$\begin{aligned}\dot{V}_1(t) \le& -k_{11}s_1^2 - k_{13}V_{U1} - \sigma_{w_1}\tilde{W}_1^T\hat{W}_1\\ &+ \frac{\varepsilon_1^{*2}}{2} + s_1\left[p_{10}v_{1h} - d_1[v_1](t)\right]\\ &+ \frac{1}{\eta_1}\int_0^R \tilde{p}_1(t,r)\frac{\partial}{\partial t}\hat{p}_1(t,r)dr.\end{aligned} \quad (43)$$

For the third term in (43), by completion of squares, we have

$$-\sigma_{w_1}\tilde{W}_1^T\hat{W}_1 \le -\frac{\sigma_{w_1}}{2}\|\tilde{W}_1\|^2 + \frac{\sigma_{w_1}}{2}\|W_1^*\|^2. \tag{44}$$

For the last two terms in (43), using (2) and (29), we have

$$\begin{aligned}
s_1&\left[p_{10}v_{1h} - d_1[v_1](t)\right] + \frac{1}{\eta_1}\int_0^R \tilde{p}_1(t,r)\frac{\partial}{\partial t}\hat{p}_1(t,r)dr \\
&= s_1\left[-\frac{\text{sgn}(s_1)p_{10}}{p_{10\min}}\int_0^R \hat{p}_1(t,r)\left|F_{1r}[v](t)\right|dr - \int_0^R p_1(r)F_{1r}[v](t)dr\right] \\
&\quad + \frac{1}{\eta_1}\int_0^R \tilde{p}_1(t,r)\frac{\partial}{\partial t}\hat{p}_1(t,r)dr \\
&\le -|s_1|\int_0^R \hat{p}_1(t,r)\left|F_{1r}[v](t)\right|dr \\
&\quad + |s_1|\int_0^R p_1(r)\left|F_{1r}[v](t)\right|dr \\
&\quad + \frac{1}{\eta_1}\int_0^R \tilde{p}_1(t,r)\frac{\partial}{\partial t}\hat{p}_1(t,r)dr \\
&\le -|s_1|\int_0^R \tilde{p}_1(t,r)\left|F_{1r}[v](t)\right|dr \\
&\quad + \frac{1}{\eta_1}\int_0^R \tilde{p}_1(t,r)\frac{\partial}{\partial t}\hat{p}_1(t,r)dr.
\end{aligned} \tag{45}$$

According to (33), the adaptation law for the estimate of density function $\hat{p}_1(t,r)$ is divided into two cases, due to the different regions which $\hat{p}_1(t,r)$ belongs to. Therefore, we also need to consider two cases for the analysis of (45).

a) $r \in R_{1\max} = \{r : \hat{p}_1(t,r) \ge p_{1\max}\} \subset [0,R]$.
According to (33), we have

$$\tilde{p}_1(t,r) \ge 0 \tag{46}$$

$$\frac{\partial}{\partial t}\hat{p}_1(t,r) = -\eta_1\sigma_{p_1}\hat{p}_1(t,r). \tag{47}$$

Substituting (46) and (47) into (45), we have

$$\begin{aligned}
-|s_1|&\int_{r\in R_{1\max}} \tilde{p}_1(t,r)\left|F_{1r}[v](t)\right|dr \\
&+ \frac{1}{\eta_1}\int_{r\in R_{1\max}} \tilde{p}_1(t,r)\frac{\partial}{\partial t}\hat{p}_1(t,r)dr \\
&\le -\sigma_{p_1}\int_{r\in R_{1\max}} \tilde{p}_1(t,r)\hat{p}_1(t,r)dr.
\end{aligned} \tag{48}$$

b) $r \in R_{1\max}^c$, which is the complement set of $R_{1\max}$ in $[0,R]$, i.e., $0 \le \hat{p}_1(t,r) < p_{1\max}$.
In this case, from (33), we have

$$\frac{\partial}{\partial t}\hat{p}_1(t,r) = \eta_1\left[|s_1|\left|F_{1r}[v_1](t)\right| - \sigma_{p_1}\hat{p}_1(t,r)\right] \tag{49}$$

Substituting (49) into (45), we have

$$\begin{aligned}
-|s_1|&\int_{r\in R_{1\max}^c} \tilde{p}_1(t,r)\left|F_{1r}[v](t)\right|dr \\
&+ \frac{1}{\eta_1}\int_{r\in R_{1\max}^c} \tilde{p}_1(t,r)\frac{\partial}{\partial t}\hat{p}_1(t,r)dr \\
&\le -\sigma_{p_1}\int_{r\in R_{1\max}^c} \tilde{p}_1(t,r)\hat{p}_1(t,r)dr.
\end{aligned} \tag{50}$$

Combining (45), (48), and (50), we know that

$$\begin{aligned}
s_1&\left[p_{10}v_{1h} - d_1[v_1](t)\right] \\
&+ \frac{1}{\eta_1}\int_0^R \tilde{p}_1(t,r)\frac{\partial}{\partial t}\hat{p}_1(t,r)dr \\
&\le -\sigma_{p_1}\int_0^R \tilde{p}_1(t,r)\hat{p}_1(t,r)dr.
\end{aligned} \tag{51}$$

By completion of squares, we have

$$-\sigma_{p_1}\tilde{p}_1(t,r)\hat{p}_1(t,r) \le -\frac{\sigma_{p_1}}{2}\tilde{p}_1^2(t,r) + \frac{\sigma_{p_1}}{2}p_1^2(r). \tag{52}$$

Integrating both sides of (52) over $[0,R]$ results in

$$\begin{aligned}
-\sigma_{p_1}&\int_0^R \tilde{p}_1(t,r)\hat{p}_1(t,r)dr \\
&\le -\frac{\sigma_{p_1}}{2}\int_0^R \tilde{p}_1^2(t,r)dr + \frac{\sigma_{p_1}}{2}\int_0^R p_1^2(r)dr.
\end{aligned} \tag{53}$$

According to Assumption 4, we know that $p_1(r) \le p_{1\max}$. Therefore

$$\begin{aligned}
-\sigma_{p_1}&\int_0^R \tilde{p}_1(t,r)\hat{p}_1(t,r)dr \\
&\le -\frac{\sigma_{p_1}}{2}\int_0^R \tilde{p}_1^2(t,r)dr + \frac{\sigma_{p_1}R}{2}p_{1\max}^2.
\end{aligned} \tag{54}$$

Substituting (44), (51), and (54) into (43), we have

$$\begin{aligned}
\dot{V}_1(t) \le& -k_{11}s_1^2 - k_{13}V_{U1} - \frac{\sigma_{w_1}}{2}\|\tilde{W}_1\|^2 \\
&- \frac{\sigma_{p_1}}{2}\int_0^R \tilde{p}_1^2(t,r)dr + \frac{\sigma_{p_1}R}{2}p_{1\max}^2 \\
&+ \frac{\sigma_{w_1}}{2}\|W_1^*\|^2 + \frac{\varepsilon_1^{*2}}{2} \\
\le& -\lambda_{11}V_1(t) + \mu_{11}
\end{aligned} \tag{55}$$

where

$$\lambda_{11} = \min\left\{\frac{b_{10}k_{11}}{\lambda_{s1}}, k_{13}, \frac{\sigma_{w_1}}{\lambda_{\max}\left(\Gamma_1^{-1}\right)}, \sigma_{p_1}\eta_1\right\}$$

$$\mu_{11} = \frac{\sigma_{p_1}R}{2}p_{1\max}^2 + \frac{\sigma_{w_1}}{2}\|W_1^*\|^2 + \frac{\varepsilon_1^{*2}}{2}.$$

Multiplying (55) by $e^{\lambda_{11}t}$ and integrating over $[0, t]$, we have

$$0 \le V_1(t) \le \frac{\mu_{11}}{\lambda_{11}} + \left[V_1(0) - \frac{\mu_{11}}{\lambda_{11}}\right]e^{-\lambda_{11}t} \le \mu_1 \quad (56)$$

where $\mu_1 = (\mu_{11}/\lambda_{11}) + V_1(0)$. Therefore, according to the definition of $V_1(t)$ in (38), $\|\tilde{W}_1\| \le \sqrt{2\mu_1/\lambda_{\min}(\Gamma_1^{-1})}$ and $|s_1| \le \sqrt{2b_{11}V_1(t)} \le \sqrt{2b_{11}\mu_1}$.

- **Region 2**: If $|s_1| < c_{s_1}$, then $q_1(s_1|c_{s_1}) = 0$. In this case, the control signal $v_1 = 0$, $v_{1h} = 0$, $\dot{\hat{W}}_1 = 0$, $(\partial/\partial t)\hat{p}_1(t, r) = 0$, i.e., all the signals are kept bounded.

Define $\pi_1 = [e_{11}, \ldots, e_{1,n_1-1}]^T \in R^{n_1-1}$. From (12), we know that 1) there is a state–space representation for mapping $s_1 = [\Lambda^T\ 1]e_1$, i.e., $\dot{\pi}_1 = A_{s_1}\pi_1 + b_{s_1}s_1$ with $\Lambda_1 = [\lambda_{11}, \ldots, \lambda_{1,n_1-1}]^T$, $b_{s_1} = [0, \ldots, 0, 1]^T$, A_{s_1} being a stable matrix; 2) there are positive constants c_{10} and λ_1 such that $\|e^{A_{s_1}t}\| \le c_{10}e^{-\lambda_1 t}$, and 3) the solution of π_1 is

$$\pi_1(t) = e^{A_{s_1}t}\pi_1(0) + \int_0^t e^{A_{s_1}(t-\tau)}b_{s_1}s_1(\tau)d\tau.$$

Accordingly, it follows that

$$\begin{aligned}\|\pi_1(t)\| &\le c_{10}\|\pi_1(0)\|e^{-\lambda_1 t} + c_{10}\int_0^t e^{-\lambda_1(t-\tau)}|s_1(\tau)|d\tau\\ &\le c_{10}\|\pi_1(0)\| + \frac{c_{10}\sqrt{2b_{11}\mu_1}}{\lambda_1}. \quad (57)\end{aligned}$$

Noting $s_1 = \Lambda_1^T\pi_1 + e_{1n_1}$ and $e_1 = [\pi_1^T, e_{1n_1}]^T$, we have

$$\|e_1\| \le \|\pi_1\| + |e_{1n_1}| \le (1 + \|\Lambda_1\|)\|\pi_1\| + |s_1|.$$

Substituting (57) into the above inequality leads to

$$\|e_1\| \le c_{10}(1+\|\Lambda_1\|)\|\pi_1(0)\| + \left[1 + \frac{(1+\|\Lambda_1\|)c_{10}}{\lambda_1}\right]\sqrt{2b_{11}\mu_1}.$$

Therefore, we can conclude that all the closed-loop signals are SGUUB for some initial conditions, and the tracking error will converge to a neighborhood of zero.

Furthermore, from (56), we also can have

$$0 \le V_1(t) \le \mu_1^*, \quad t \to \infty \quad (58)$$

where $\mu_1^* = \mu_{11}/\lambda_{11}$. Therefore, $\|\tilde{W}_1\| \le \sqrt{2\mu_1^*/\lambda_{\min}(\Gamma_1^{-1})}$ and $|s_1| \le \sqrt{2b_{11}V_1(t)} \le \sqrt{2b_{11}\mu_1^*}$, as $t \to \infty$.

Step 2: In this step, we prove that there exist some control parameters and a nonempty initial compact set Ω_{10}, such that as long as initial conditions belong in Ω_{10}, the states and the weights under the proposed control, for $t > 0$, will never escape from the conservative compact set Ω_1, which belongs to the chosen compact set $\Omega_{\rm NN}$, as shown in Fig. 2.

From the definition of the bounds of the compact sets Ω_1 in (34) and Ω_{1s} in (37), we can see that for a given $\Omega_{\rm NN}$, there exist some $V_1(0)$, μ_{11}, λ_{11} such that $\Omega_1 \subset \Omega_{\rm NN}$ and $\Omega_{1s} \subset \Omega_{\rm NN}$. From the definitions of μ_{11} and λ_{11} in (35) and (36) as follows

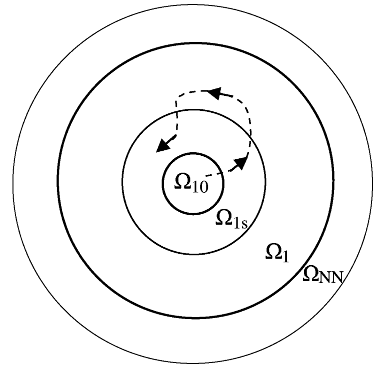

Fig. 2. Compact sets.

$$\mu_{11} = \frac{\sigma_{p_1}R}{2}p_{1\max}^2 + \frac{\sigma_{w_1}}{2}\|W_1^*\|^2 + \frac{\varepsilon_1^{*2}}{2}$$

$$\lambda_{11} = \min\left\{\frac{b_{10}k_{11}}{\lambda_{s1}}, k_{13}, \frac{\sigma_{w_1}}{\lambda_{\max}\left(\Gamma_1^{-1}\right)}, \sigma_{p_1}\eta_1\right\}$$

we can see that the values of μ_{11} and λ_{11} depend on the choice of the control parameters k_{11}, k_{13}, $\lambda_{\max}(\Gamma_1^{-1})$, and η_1. Therefore, for a given NN compact set $\Omega_{\rm NN}$, there exist some control parameters such that $\Omega_1 \subset \Omega_{\rm NN}$ for a $V(0) = V_{\max} > 0$. Then, we define the initial compact set Ω_{10} as the set of initial conditions $s_1(0), \hat{W}_1(0)$ such that $V(0) < V_{\max}$. Therefore, for all $s_1(0), \hat{W}_1(0)$ that belong to Ω_{10}, we have $\Omega_1 \subset \Omega_{\rm NN}$ for $t > 0$. If Ω_1 and Ω_{1s} are larger than $\Omega_{\rm NN}$, this means that the initial conditions do not belong to a valid initial compact set Ω_{10}. This completes the proof. ∎

B. *Adaptive NN Control for MIMO Case* $(m \ge 2)$

In the foregoing discussions, we design control for the SISO case by Lyapunov synthesis design, so as to elucidate the main ideas of our control design. In this section, we extend the previous result to the MIMO case (4). System (4) is block triangular with respect to inputs u, as seen in the fact that nonlinearities $f_i(x, \bar{u}_{i-1})$ only contain inputs from the preceding subsystems. This structure of interconnection facilitates systematic recursive design.

Substituting (4) into (12) leads to

$$\begin{aligned}\dot{s}_i = f_i(x, \bar{u}_{i-1}) &+ g_{i,\tau}\left(x_1\left(t - \tau_1(t)\right), \ldots, x_m\left(t - \tau_m(t)\right)\right)\\ &+ b_i(\bar{x}_i)p_{i0}v_i(t) - b_i(\bar{x}_i)d_i[v_i](t) + \nu_i \quad (59)\end{aligned}$$

where $\nu_i = \sum_{j=1}^{n_i-1}\lambda_{ij}e_{i,j+1} - y_{id}^{(n_i)}$.

Define the following integral Lyapunov function candidate:

$$V_{si} = \int_0^{s_i}\frac{\sigma}{b_i\left(\bar{x}_i^+, \sigma + \beta_i\right)}d\sigma \quad (60)$$

where $\beta_i = y_{id}^{(n_i-1)} - \sum_{j=1}^{n_i-1}\lambda_{ij}e_{ij}$, and $\bar{x}_i^+ = [x_1^T, \ldots, x_{i-1}^T, x_{i,1}, \ldots, x_{i,n_i-1}]^T$. Applying the first mean value theorem for integrals to (60), we have

$$V_{si} = \frac{\lambda_{si}s_i^2}{b_i\left(\bar{x}_i^+, \lambda_{si}s_i + \beta_i\right)}, \qquad \lambda_{si} \in (0, 1)$$

which is positive definite with respect to s_i due to Assumption 1, $0 < b_{i0} \leq b_i(\bar{x}_i)$.

Differentiating V_{si} with respect to time t, we obtain

$$\begin{aligned}\dot{V}_{si} &= \frac{\partial V_{si}}{\partial s_i}\dot{s}_i + \frac{\partial V_{si}}{\partial \bar{x}_i^+}\dot{\bar{x}}_i^+ + \frac{\partial V_{si}}{\partial \beta_i}\dot{\beta}_i \\ &= \frac{s_i}{b_i(\bar{x}_i)}\left[f_i(x,\bar{u}_{i-1}) + g_{i,\tau}\left(x_1\left(t-\tau_1(t)\right),\ldots,x_m\left(t-\tau_m(t)\right)\right) + b_i(\bar{x}_i)p_{i0}v_i(t) - b_i(\bar{x}_i)d_i[v_i](t) + \nu_i\right] \\ &\quad + \sum_{j=1}^{i-1} g_{i,\tau}\left(x_1\left(t-\tau_1(t)\right),\ldots,x_m\left(t-\tau_m(t)\right)\right) \times \int_0^{s_i}\sigma\left[\frac{\partial b_i^{-1}\left(\bar{x}_i^+,\sigma+\beta_i\right)}{\partial x_{jn_j}}\right]d\sigma \\ &\quad + \int_0^{s_i}\sigma\left\{\sum_{j=1}^{i}\sum_{k=1}^{n_j-1}\frac{\partial b_i^{-1}\left(\bar{x}_i^+,\sigma+\beta_i\right)}{\partial x_{jk}}x_{j,k+1} + \sum_{j=1}^{i-1}\frac{\partial b_i^{-1}\left(\bar{x}_i^+,\sigma+\beta_i\right)}{\partial x_{jn_j}} \times \left[f_j(x,\bar{u}_{i-1}) + b_j(\bar{x}_j)u_j(v_j)\right]\right\}d\sigma \\ &\quad - \frac{\nu_i s_i}{b_i(\bar{x}_i)} + \int_0^{s_i}\frac{\nu_i}{b_i\left(\bar{x}_i^+,\sigma+\beta_i\right)}d\sigma. \end{aligned} \tag{61}$$

Using (10), after some manipulations, (61) becomes

$$\begin{aligned}\dot{V}_{si} &\leq s_iQ_i + s_i\left[p_{i0}v_i(t) - d_i[v_i](t)\right] + \frac{|s_i|}{|b_i(\bar{x}_i)|}\sum_{k=1}^{m}\varrho_{ik}\left(x_k\left(t-\tau_k(t)\right)\right) \\ &\quad + \sum_{j=1}^{i-1}\sum_{k=1}^{m}\varrho_{jk}\left(x_k\left(t-\tau_k(t)\right)\right)s_i^2 \times \int_0^1\theta\left[\frac{\partial b_i^{-1}\left(\bar{x}_i^+,\theta s_i+\beta_i\right)}{\partial x_{jn_j}}\right]d\theta \end{aligned} \tag{62}$$

where

$$\begin{aligned}Q_i(Z_i) &= \frac{f_i(x,\bar{u}_{i-1})}{b_i(\bar{x}_i)} + \int_0^1\left\{\theta s_i\left[\sum_{j=1}^{i}\sum_{k=1}^{n_j-1}\frac{\partial b_i^{-1}\left(\bar{x}_i^+,\sigma+\beta_i\right)}{\partial x_{jk}}x_{j,k+1} + \sum_{j=1}^{i-1}\frac{\partial b_i^{-1}\left(\bar{x}_i^+,\theta s_i+\beta_i\right)}{\partial x_{jn_j}} \times \left[f_j(x,\bar{u}_{i-1}) + b_j(\bar{x}_j)u_j(v_j)\right]\right] + \frac{\nu_i}{b_i\left(\bar{x}_i^+,\theta s_i+\beta_i\right)}\right\}d\theta\end{aligned}$$

with $Z_i = \left[x^T, s_i, \nu_i, \beta_i, v_1, \ldots, v_{i-1}\right]^T \in R^{(\sum_{i=1}^{m} n_i)+i+2}$.

By utilizing Young's inequality, we obtain that

$$\frac{|s_i|}{|b_i(\bar{x}_i)|}\sum_{k=1}^{m}\varrho_{ik}\left(x_k\left(t-\tau_k(t)\right)\right) \leq \frac{ms_i^2}{2b_i^2(\bar{x}_i)} + \frac{1}{2}\sum_{k=1}^{m}\varrho_{ik}^2\left(x_k\left(t-\tau_k(t)\right)\right) \tag{63}$$

and

$$\begin{aligned}&\sum_{j=1}^{i-1}\sum_{k=1}^{m}\varrho_{jk}\left(x_k\left(t-\tau_k(t)\right)\right)s_i^2\int_0^1\theta\left[\frac{\partial b_i^{-1}\left(\bar{x}_i^+,\theta s_i+\beta_i\right)}{\partial x_{jn_j}}\right]d\theta \\ &\leq \frac{1}{2}\sum_{j=1}^{i-1}\sum_{k=1}^{m}\varrho_{jk}^2\left(x_k\left(t-\tau_k(t)\right)\right) + \frac{ms_i^4}{2}\sum_{j=1}^{i-1}\left(\int_0^1\theta\left[\frac{\partial b_i^{-1}\left(\bar{x}_i^+,\theta s_i+\beta_i\right)}{\partial x_{jn_j}}\right]d\theta\right)^2. \end{aligned} \tag{64}$$

Substituting (63) and (64) into (62), we have

$$\begin{aligned}\dot{V}_{si} &\leq s_iQ_i + s_i\left[p_{i0}v_i(t) - d_i[v_i](t)\right] + \frac{ms_i^2}{2b_i^2(\bar{x}_i)} + \frac{1}{2}\sum_{j=1}^{i}\sum_{k=1}^{m}\varrho_{jk}^2\left(x_k\left(t-\tau_k(t)\right)\right) \\ &\quad + \frac{ms_i^4}{2}\sum_{j=1}^{i-1}\left(\int_0^1\theta\left[\frac{\partial b_i^{-1}\left(\bar{x}_i^+,\theta s_i+\beta_i\right)}{\partial x_{jn_j}}\right]d\theta\right)^2. \end{aligned} \tag{65}$$

To overcome the design difficulties from the unknown time-varying delays $\tau_1(t),\ldots,\tau_m(t)$ in (65), the following Lyapunov–Krasovskii functional can be considered:

$$V_{U_i}(t) = \frac{1}{2(1-\bar{\tau}_{\max})}\sum_{j=1}^{i}\sum_{k=1}^{m}\int_{t-\tau_k(t)}^{t}\varrho_{jk}^2\left(x_k(\tau)\right)d\tau. \tag{66}$$

The time derivative of V_{U_i} can be expressed as follows:

$$\dot{V}_{U_i}(t) = \frac{1}{2(1-\bar{\tau}_{\max})}\left[\sum_{j=1}^{i}\sum_{k=1}^{m}\varrho_{jk}^2\left(x_k(t)\right) - \sum_{j=1}^{i}\sum_{k=1}^{m} \varrho_{jk}^2\left(x_k\left(t-\tau_k(t)\right)\right)\left(1-\dot{\tau}_k(t)\right)\right] \tag{67}$$

which can be used to cancel the time delay term on the right-hand side of (65).

Combining (65) and (67), we obtain

$$\dot{V}_{si} + \dot{V}_{Ui} \leq s_ih_i(Z_i) + s_i\left[p_{i0}v_i(t) - d_i[v_i](t)\right] \tag{68}$$

where

$$\begin{aligned}h_i(Z_i) &= Q_i(Z_i) + \frac{ms_i}{2b_i^2(\bar{x}_i)} + \frac{1}{2(1-\bar{\tau}_{\max})s_i}\sum_{j=1}^{i}\sum_{k=1}^{m}\varrho_{jk}^2\left(x_k(t)\right) \\ &\quad + \frac{ms_i^3}{2}\sum_{j=1}^{i-1}\left(\int_0^1\theta\left[\frac{\partial b_i^{-1}(\bar{x}_i^+,\theta s_i+\beta_i)}{\partial x_{jn_j}}\right]d\theta\right)^2. \end{aligned} \tag{69}$$

Define the following compact sets:

$$\Omega_{Z_1} = \left\{[x^T, s_1, \nu_1, \beta_1]^T | x_j \in \Omega_j, j=1,\ldots,m, x_{1d} \in \Omega_{1d}\right\} \tag{70}$$

$$\Omega_{Z_i} = \Big\{[x^T, s_i, \nu_i, \beta_i, v_1, \ldots, v_{i-1}]^T | x_j \in \Omega_j, j=1,\ldots,m, x_{kd} \in \Omega_{kd}, k=1,\ldots,i, \hat{W}_j \in \Omega_j, j=1,\ldots,i-1\Big\} \tag{71}$$

$$\Omega_{c_{s_i}} = \{s_i | |s_i| < c_{s_i}, x_{id} \in \Omega_{id}\} \tag{72}$$

$$\Omega^0_{Z_i} = \Omega_{Z_i} - \Omega_{c_{s_i}} \tag{73}$$

where $\Omega_j \subset R^{n_j}$ is a sufficiently large compact set satisfying $\Omega_j \supset \Omega_{j0}$ defined in Theorem 2, and c_{s_i} is a positive design constant that can be chosen arbitrarily small. The compact set $\Omega^0_{Z_i}$ is the complement set of set $\Omega_{c_{s_i}}$.

Let $\hat{W}_i^T S(Z_i)$ be the approximation of the function $h_i(Z_i)$, defined in (69), on the compact set $\Omega^0_{Z_i}$. Then, using RBFNN as discussed in Section II-C, we have

$$h_i(Z_i) = \hat{W}_i^T S(Z_i) - \tilde{W}_i^T S(Z_i) + \varepsilon_i(Z_i) \tag{74}$$

where the approximation error $\varepsilon_i(Z_i)$ satisfies $|\varepsilon_i(Z_i)| \le \varepsilon_i^*$ with positive constant ε_i^*, $\forall Z_i \in \Omega^0_{Z_i}$.

Similar to the procedures of Section III-A, we design the following control law for the system in (4):

$$v_i = -q(s_i|c_{s_i}) \frac{\operatorname{sgn}(s_i)}{p_{i0\min}} \left[k_{i0}(t)|s_i| + \left|\hat{W}_i^T S(Z_i)\right|\right] + v_{ih} \tag{75}$$

$$v_{ih}(t) = -q(s_i|c_{s_i}) \frac{\operatorname{sgn}(s_i)}{p_{i0\min}} \int_0^R \hat{p}_i(t,r)\, |F_{ir}[v_i](t)|\, dr \tag{76}$$

$$k_{i0}(t) = q(s_i|c_{s_i}) \left[k_{i1} + k_{i2}(t) + \frac{1}{2}\right] \tag{77}$$

where $q(s_i|c_{s_i})$ is defined in (11); $\hat{p}_i(t,r)$ is the estimate of the density function $p_i(r)$; parameter k_{i1} is any positive constant and $k_{i2}(t)$ is chosen as

$$k_{i2}(t) = q(s_i|c_{s_i}) \frac{k_{i3}}{2(1-\bar{\tau}_{\max}) s_i^2} \sum_{j=1}^{i} \sum_{k=1}^{m} \int_{t-\tau_{\max}}^{t} \varrho_{jk}^2 (x_k(\tau))\, d\tau \tag{78}$$

with k_{i3} a positive constant specified by the designer.

The adaptation laws are chosen as

$$\dot{\hat{W}}_i = q(s_i|c_{s_i}) \Gamma_i \left[S(Z_i)s_i - \sigma_{w_i} \hat{W}_i\right] \tag{79}$$

$$\frac{\partial}{\partial t}\hat{p}_i(t,r) = \begin{cases} -q(s_i|c_{s_i}) \eta_i \sigma_{p_i} \hat{p}_i(t,r), \\ \qquad \text{if } \hat{p}_i(t,r) \ge p_{i\max} \\ q(s_i|c_{s_i}) \eta_i \left[|s_i| \left|F_{ir}[x_{i,n_i}](t)\right| - \sigma_{p_i}\hat{p}_i(t,r)\right], \\ \qquad \text{if } 0 \le \hat{p}_i(t,r) < p_{i\max}. \end{cases} \tag{80}$$

with $\Gamma_i > 0$, σ_{w_i}, σ_{p_i}, and η_i being strictly positive constants.

Based on the above design for control and adaptation laws, we are ready to establish the following result for the MIMO case.

Theorem 2: Consider the closed-loop system consisting of the plant (4), the control laws (75) and (76), and adaptation laws (79) and (80). Under Assumptions 1–4, given that some initial conditions $x_i(0), \hat{W}_i(0)$, belong in Ω_{i0}, we can conclude that the overall closed-loop neural control system is SGUUB in the sense that all of the signals in the closed-loop system are bounded, i.e., the states and the weights in the closed-loop system will remain in the compact set defined by

$$\Omega_i = \left\{ s_i, \tilde{W}_i | |s_i| \le \sqrt{2\mu_i}, \|\tilde{W}_i\| \le \sqrt{\frac{2\mu_i}{\lambda_{\min}\left(\Gamma_i^{-1}\right)}} \right\} \tag{81}$$

with

$$\mu_i = \frac{\mu_{i1}}{\lambda_{i1}} + V_i(0)$$

$$\mu_{i1} = \frac{\sigma_{p_i} R}{2} p_{i\max}^2 + \frac{\sigma_{w_i}}{2} \|W_i^*\|^2 + \frac{\varepsilon_i^{*2}}{2}$$

$$\lambda_{i1} = \min\left\{ \frac{b_{i0}k_{i1}}{\lambda_{si}}, k_{i3}, \frac{\sigma_{w_i}}{\lambda_{\max}\left(\Gamma_i^{-1}\right)}, \sigma_{p_i}\eta_i \right\}$$

$$V_i(0) = V_{si}(0) + V_{U_i}(0) + \frac{1}{2}\tilde{W}_i^T(0)\Gamma_i^{-1}\tilde{W}_i(0) + \frac{1}{2\eta_i}\int_0^R \tilde{p}_i^2(0,r)dr$$

and the tracking error will converge to a neighborhood of zero. In addition, the states and the weights in the closed-loop system will eventually converge to the compact set defined by

$$\Omega_{is} = \left\{ s_i, \tilde{W}_i | |s_i| \le \sqrt{2\mu_i^*}, \|\tilde{W}_i\| \le \sqrt{\frac{2\mu_i^*}{\lambda_{\min}\left(\Gamma_i^{-1}\right)}} \right\} \tag{82}$$

where

$$\mu_i^* = \frac{\mu_{i1}}{\lambda_{i1}}.$$

Proof: The proof is built on that of Theorem 1, and for the conciseness, we will only outline the general approach without going into specific details. For the ith subsystem, we design v_i that takes into account the inputs from the preceding $(i-1)$ subsystems, i.e., $\bar{v}_{i-1}$.

Suppose that both the states and the weights belong to $\Omega_{\rm NN}$, i.e., $\{x_j, \hat{W}_i\} \in \Omega_{\rm NN}, \forall t \ge 0$, on which NN approximation (74) is valid. Consider the following Lyapunov function candidate:

$$V_i(t) = V_{si}(t) + V_{U_i}(t) + \frac{1}{2}\tilde{W}_i^T\Gamma_i^{-1}\tilde{W}_i + \frac{1}{2\eta_i}\int_0^R \tilde{p}_i^2(t,r)dr \tag{83}$$

where $\tilde{W}_i = \hat{W}_i - W_i$ and $\tilde{p}_i(t,r) = \hat{p}_i(t,r) - p_i(r)$. Differentiating $V_i(t)$ with respect to time t leads to

$$\dot{V}_i(t) = \dot{V}_{si}(t) + \dot{V}_{U_i}(t) + \tilde{W}_i^T\Gamma_i^{-1}\dot{\hat{W}}_i + \frac{1}{\eta_i}\int_0^R \tilde{p}_i(t,r)\frac{\partial}{\partial t}\hat{p}_i(t,r)dr. \tag{84}$$

Substituting (68) into (84) leads to

$$\dot{V}_i(t) \le s_i h_i(Z_i) + s_i\left[p_{i0}v_i - d_i[v_i](t)\right] + \tilde{W}_i^T\Gamma_i^{-1}\dot{\hat{W}}_i + \frac{1}{\eta_i}\int_0^R \tilde{p}_i(t,r)\frac{\partial}{\partial t}\hat{p}_i(t,r)dr. \tag{85}$$

Considering the adaptive neural control laws and adaptation laws from (75)–(80), the stability analysis is carried out in the following two regions, respectively.

- **Region 1**: If $|s_i| \geq c_{s_i}$, then $q_i(s_i|c_{s_i}) = 1$. Noting (74) and submitting (75) into (85), we have

$$\begin{aligned}\dot{V}_i(t) \leq & - s_i\tilde{W}_i^T S(Z_i) + s_i\varepsilon_1(Z_i) - k_{i0}(t)s_i^2 \\ & + s_i\left[p_{i0}v_{ih} - d_i[v_i](t)\right] + \tilde{W}_i^T\Gamma_i^{-1}\dot{\hat{W}}_i \\ & + \frac{1}{\eta_i}\int_0^R \tilde{p}_i(t,r)\frac{\partial}{\partial t}\hat{p}_i(t,r)dr. \end{aligned} \quad (86)$$

Using Young's inequality, we have

$$s_i\varepsilon_i(Z_i) \leq \frac{s_i^2}{2} + \frac{\varepsilon_i^{*2}}{2}. \quad (87)$$

Substituting (77), (79), and (87) into (86) leads to

$$\begin{aligned}\dot{V}_i(t) \leq & -k_{i1}s_i^2 - k_{i3}V_{Ui} - \sigma_{w_i}\tilde{W}_i^T\hat{W}_i + \frac{\varepsilon_i^{*2}}{2} \\ & + s_i\left[p_{i0}v_{ih} - d_i[v_i](t)\right] \\ & + \frac{1}{\eta_i}\int_0^R \tilde{p}_i(t,r)\frac{\partial}{\partial t}\hat{p}_i(t,r)dr. \end{aligned} \quad (88)$$

For the third term in (88), by completion of squares, we have

$$-\sigma_{w_i}\tilde{W}_i^T\hat{W}_i \leq -\frac{\sigma_{w_i}}{2}\|\tilde{W}_i\|^2 + \frac{\sigma_{w_i}}{2}\|W_i^*\|^2. \quad (89)$$

For the last two terms in (88), we can obtain the similar conclusions as (51) and (54)

$$\begin{aligned} & s_i\left[p_{i0}v_{ih} - d_i[v_i](t)\right] + \frac{1}{\eta_i}\int_0^R \tilde{p}_i(t,r)\frac{\partial}{\partial t}\hat{p}_i(t,r)dr \\ & \leq -\sigma_{p_i}\int_0^R \tilde{p}_i(t,r)\hat{p}_i(t,r)dr \\ & \leq -\frac{\sigma_{p_i}}{2}\int_0^R \tilde{p}_i^2(t,r)dr + \frac{\sigma_{p_i}R}{2}p_{i\max}^2. \end{aligned} \quad (90)$$

Substituting (89) and (90) into (88), we have

$$\begin{aligned}\dot{V}_i(t) \leq & -k_{i1}s_1^2 - k_{i3}V_{Ui} - \frac{\sigma_{w_i}}{2}\|\tilde{W}_i\|^2 \\ & - \frac{\sigma_{p_i}}{2}\int_0^R \tilde{p}_i^2(t,r)dr \\ & + \frac{\sigma_{p_i}R}{2}p_{i\max}^2 + \frac{\sigma_{w_i}}{2}\|W_i^*\|^2 + \frac{\varepsilon_i^{*2}}{2} \\ \leq & -\lambda_{i1}V_i(t) + \mu_{i1} \end{aligned} \quad (91)$$

where

$$\lambda_{i1} = \min\left\{\frac{b_{i0}k_{i1}}{\lambda_{si}}, k_{i3}, \frac{\sigma_{w_i}}{\lambda_{\max}\left(\Gamma_i^{-1}\right)}, \sigma_{p_i}\eta_i\right\}$$

$$\mu_{i1} = \frac{\sigma_{p_i}R}{2}p_{i\max}^2 + \frac{\sigma_{w_i}}{2}\|W_i^*\|^2 + \frac{\varepsilon_i^{*2}}{2}.$$

Multiplying (91) by $e^{\lambda_{i1}t}$ and integrating over $[0,t]$, we have

$$0 \leq V_i(t) \leq \frac{\mu_{i1}}{\lambda_{i1}} + \left[V_i(0) - \frac{\mu_{i1}}{\lambda_{i1}}\right]e^{-\lambda_{i1}t} \leq \mu_i \quad (92)$$

where $\mu_i = (\mu_{i1}/\lambda_{i1}) + V_i(0)$. Therefore, $\|\tilde{W}_i\| \leq \sqrt{2\mu_i/\lambda_{\min}(\Gamma_i^{-1})}$ and $|s_i| \leq \sqrt{2b_{i1}V_i(t)} \leq \sqrt{2b_{i1}\mu_i}$.

- **Region 2**: If $|s_i| < c_{s_i}$, then $q_i(s_i|c_{s_i}) = 0$. In this case, the control signal $v_i = 0$, $v_{ih} = 0$, $\dot{\hat{W}}_i = 0$, $(\partial/\partial t)\hat{p}_i(t,r) = 0$, i.e., all the signals are kept bounded.

Similar to the discussion in Theorem 1, we can conclude that the overall closed-loop neural control system is SGUUB in the sense that all of the signals in the closed-loop system are bounded, i.e., the states and the weights in the closed-loop system will remain in the compact set Ω_i defined in (81), and will eventually converge to the compact set Ω_{is} defined in (82). This completes the proof. ■

IV. Simulation Studies

In this section, results of extensive simulation studies are presented to demonstrate the effectiveness of the proposed adaptive NN approach to deal with uncertain nonlinear systems under the effects of time delay and hysteresis. For clear illustration, we consider first a simplified SISO plant with first-order dynamics, and study the tracking performance of the controller, as well as perform detailed analysis on the effects of control parameter variations. Subsequently, a MIMO plant consisting of two interconnected second-order subsystems is tackled, and the closed-loop properties and tracking behavior are investigated.

A. SISO Case

For the SISO case, we consider the following first-order scalar nonlinear system with hysteresis and state delay:

$$S_1 : \begin{cases} \dot{x} = \dfrac{1 - e^{-x}}{1 + e^{-x}} + 0.1x\left(t - \tau(t)\right) + u \\ y = x \end{cases} \quad (93)$$

where y is the plant output; u is the plant input and the output of the PI hysteresis model as in (1): $u = p_0 v - \int_0^R p(r)F_r[v](t)dr$, with $p(r) = 0.35e^{-0.003(r-1)^2}$ for $r \in [0, 100]$, $p_{\max} = 0.35$, and $p_{0\min} = 0.35$; and the time-varying delay $\tau(t) = 1 - 0.5\cos(t)$, $\tau_{\max} = 2$, and $\bar{\tau}_{\max} = 0.6$. The objective is to design control v such that the output y can track the desired trajectory $y_d = \sin(2t) + 0.1\cos(6.7t)$.

We adopt the control law and adaption laws designed in Section III-A in the following:

$$v = -q(s|c_s)\frac{\mathrm{sgn}(s)}{p_{0\min}}\left[k_0(t)|s| + \left|\hat{W}^T S(Z)\right|\right] + v_h \quad (94)$$

$$v_h = -q(s|c_s)\frac{\mathrm{sgn}(s)}{p_{0\min}}\int_0^R \hat{p}(t,r)\left|F_r[v](t)\right|dr \quad (95)$$

$$k_0(t) = q(s|c_s)\left[k_1 + k_2(t) + \frac{1}{2}\right] \quad (96)$$

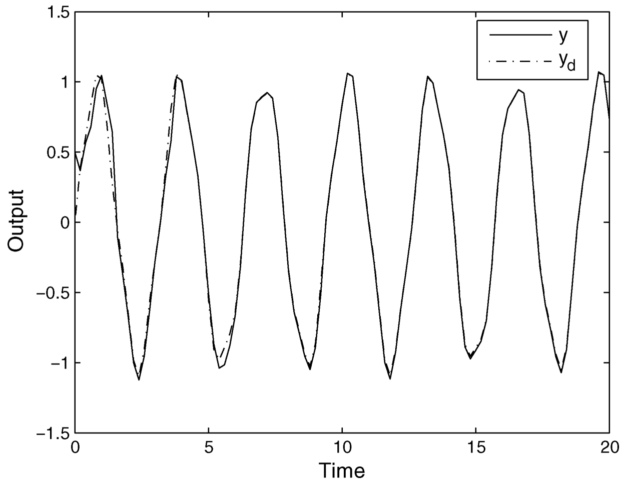

Fig. 3. Output tracking performance of SISO plant S_1.

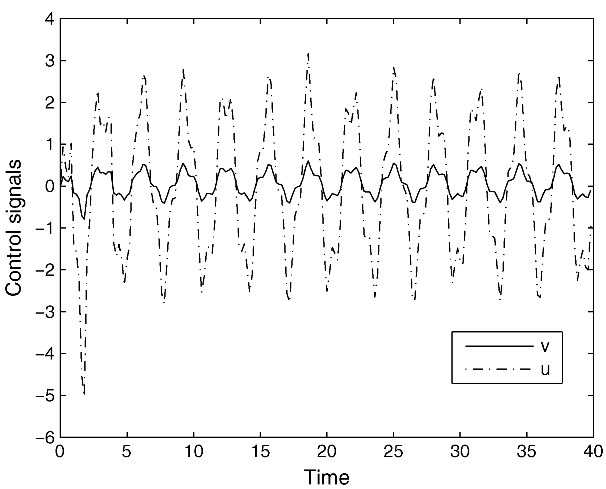

Fig. 4. Control signals of SISO plant S_1.

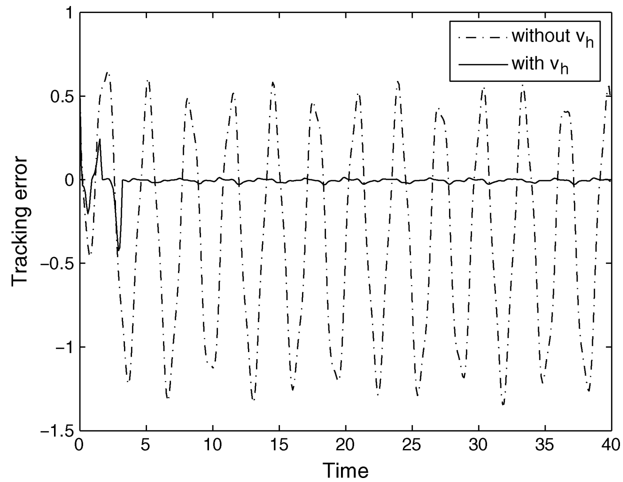

Fig. 5. Tracking error comparison result of SISO plant S_1 with and without v_h.

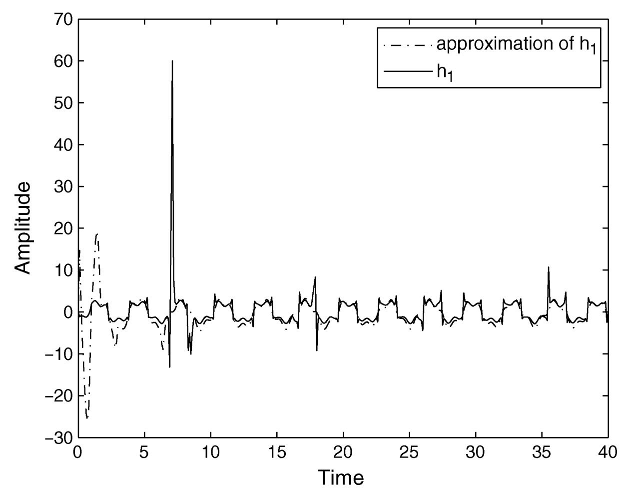

Fig. 6. Learning behavior of NNs of SISO plant S_1.

$$k_2(t)=q(s|c_s)\frac{k_3}{2(1-\bar{\tau}_{\max})s^2}\int_{t-\tau_{\max}}^{t}\varrho^2\left(x(\tau)\right)d\tau \tag{97}$$

$$\dot{\hat{W}}=q(s|c_s)\Gamma_1\left[S(Z)s-\sigma_w\hat{W}\right] \tag{98}$$

$$\frac{\partial}{\partial t}\hat{p}(t,r)=\begin{cases}-q(s|c_s)\eta\sigma_p\hat{p}(t,r), & \text{if } \hat{p}(t,r)\geq p_{\max}\\ q(s|c_s)\eta\left[|s|\left|F_r[v](t)\right|-\sigma_p\hat{p}(t,r)\right], & \\ \quad \text{if } 0\leq\hat{p}(t,r)<p_{\max}\end{cases} \tag{99}$$

where $s=e=y-y_d$, and $\hat{p}(t,r)$ is the estimate of the density function of $p(r)$. The input of the NNs is $Z=[x,\dot{y}_d]\in R^2$. Employing ten nodes for each input dimension, we end up with $10^2=100$ nodes for the network $\hat{W}^TS(Z)$. The bounding function for the time-delay term is chosen as $\varrho(x(\tau))=0.1|x(\tau)|$, and the following initial conditions and controller design parameters are adopted in the simulation: $x(0)=0.5, v(0)=0, \hat{p}(0,r)=0, \hat{W}(0)=0, \Gamma=\text{diag}\{1.0\}$, $\sigma=0.1$, $\eta=0.2$, $\sigma_p=0.05$, $k_1=0.1$, $k_3=0.001$, $\epsilon=0.05$, and $c_s=0.0001$.

The simulation results for SISO plant S_1, as described in (93), are shown in Figs. 3–12. From Fig. 3, we can observe that good tracking performance is achieved. At the same time, the boundedness of the control signals are shown in Fig. 4. It is noted that there is a large difference between v and u, indicating the significant hysteresis effect. In particular, we highlight the importance of the term v_h in (94), which is used to mitigate the effect caused by the hysteresis term $\int_0^R p(r)F_r[v](t)dr$ in PI hysteresis model $u=p_0v-\int_0^R p(r)F_r[v](t)dr$, as discussed in Remark 8. The comparison of tracking errors in the presence and absence of v_h is shown in Fig. 5, and it is seen that with v_h, the tracking error resulting from hysteresis is attenuated accordingly. Figs. 6 and 7 show the nonlinear approximation capability of NNs $\hat{W}^TS(Z)$ and the norm of NN weights, respectively. The behavior of the estimate of the density function $\hat{p}(t,r)$ is also indicated in Fig. 8.

To investigate the effects of the control parameters on the tracking performance, and to provide recommendations for their selection, we provide the following comparison results for the design constants k_1 and η in Figs. 9 and 10. First, as shown in Fig. 9, the tracking error can be reduced by increasing the parameter k_1. Second, from (99) and Fig. 10, we know that higher learning rate, i.e., increase of η, results in better

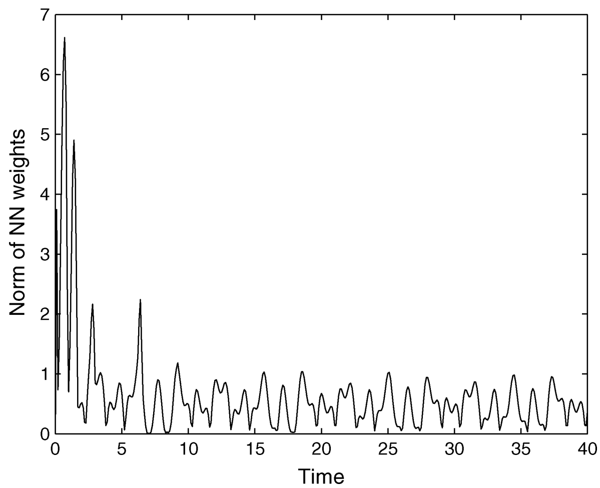

Fig. 7. Norm of NN weights of SISO plant S_1.

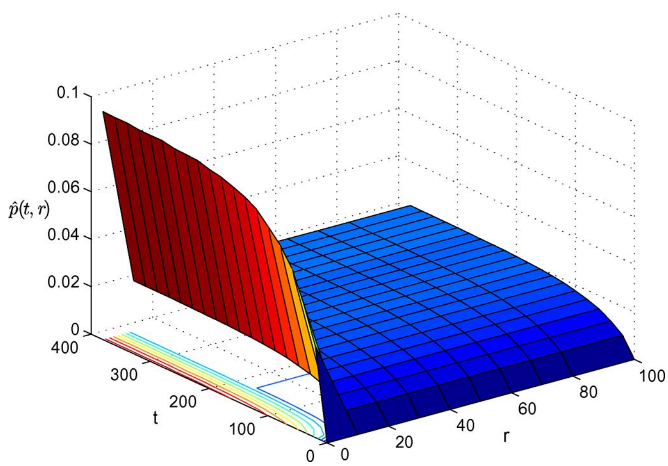

Fig. 8. Behavior of the estimate values of the density function $\hat{p}(t,r)$.

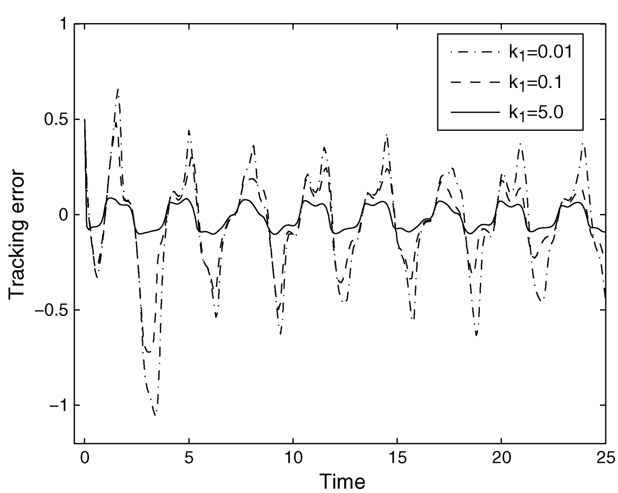

Fig. 9. Tracking error comparison result of SISO plant S_1 for different k_1.

tracking performance. While the above results seem to indicate that k_1 and η should be large, caution must be exercised in the choice of these parameters, due to the fact that there are some tradeoffs between the control performance and other issues. In particular, for the case of control gain k_1, the price to be paid is the high gain control, which also can be seen from (94) and (96). Problems associated with high gain control include sensitivity

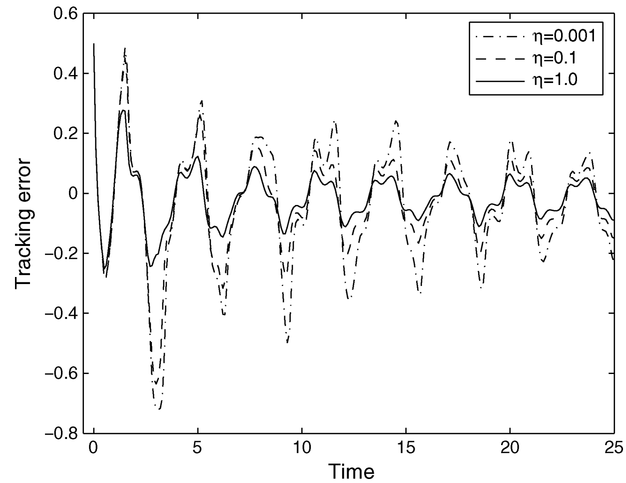

Fig. 10. Tracking error comparison result of SISO plant S_1 for different η.

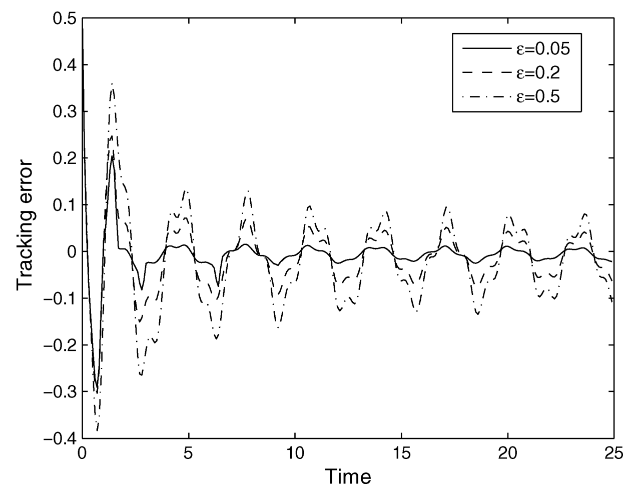

Fig. 11. Tracking error comparison result of SISO plant S_1 for different ϵ.

to measurement noise, excitation of high-frequency unmodeled dynamics, as well as excessive control efforts. A similar tradeoff exists with regard to the parameter η, which represents the learning rate of the density function estimate $\hat{p}(t,r)$, in (99). In general, if η is chosen to be too large, then the stability and the robustness of the system may be compromised in a similar way as high gain control.

We need to mention that, due to the use of sign function $\mathrm{sgn}(\cdot)$, controllers (94) and (95) become discontinuous, which may excite unmodeled high-frequency plant dynamics and cause the chattering phenomenon. To avoid the undesired chattering phenomenon, we replace the sign function in the above control laws with the saturation function $\mathrm{sat}(s/\epsilon)$, which is defined as

$$\mathrm{sat}(*) = \begin{cases} 1, & \text{if } * \geq \epsilon \\ \dfrac{*}{\epsilon}, & \text{if } |*| < \epsilon \\ -1, & \text{if } * > \epsilon \end{cases} \tag{100}$$

where ϵ is a very small positive constant. Therefore, the different choices of ϵ also can affect the tracking performance, as shown in Fig. 11. The smaller ϵ, the closer is the saturation function

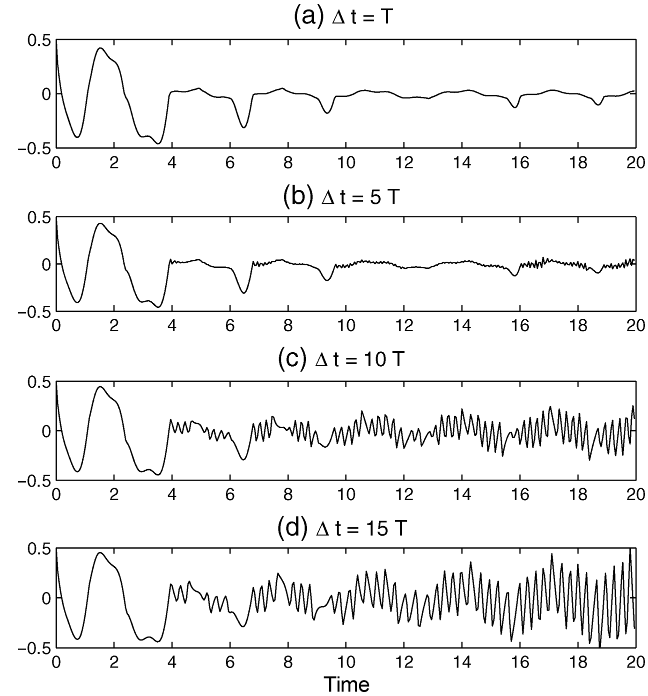

Fig. 12. We introduce a small delay Δt into $v(t)$ in calculating v_h (95) to implement the control $v(t)$ (94) numerically as pointed in Remark 9. Different Δt have different effects on the tracking performance, where $T = 0.005$ is the sampling time: (a) $\Delta t = T$; (b) $\Delta t = 5T$; (c) $\Delta t = 10T$; and (d) $\Delta t = 15T$.

approximate to the sign function. As such, though the better tracking performance can be achieved with the smaller ϵ, the chattering phenomenon will become more serious, as a result, which degrades the performance finally.

In addition, as discussed in Remark 9, we adopt a numerical method by introducing a small delay Δt to implement the control v in (94) instead of solving it directly. The choices of the delay Δt affect the performance as shown in Fig. 12. With the increasing of Δt, the performance becomes worse. In this paper, we choose $\triangle t = T$, where $T = 0.005$ is the sampling time.

B. MIMO Case

Consider the following MIMO nonlinear system consisting of two interconnected second-order subsystems with time delay and hysteresis:

$$S_2 : \begin{cases} \dot{x}_{11} = x_{12} \\ \dot{x}_{12} = x_{11}x_{12} + u_1 + 0.1x_{11}\left(t - \tau_1(t)\right) \\ \dot{x}_{21} = x_{22} \\ \dot{x}_{22} = x_{11}x_{21} + u_2 + 0.2x_{21}\left(t - \tau_2(t)\right) \\ y_1 = x_{11} \\ y_2 = x_{21} \end{cases} \tag{101}$$

where y_i are the plant outputs, $i = 1, 2$; u_i are the plant inputs and the outputs of the PI hysteresis model as in (1): $u_i = p_0 v_i - \int_0^R p(r)F_r[v_i](t)dr$ with $p(r) = 0.08e^{-0.0024(r-1)^2}$ for $r \in [0, 100]$, $p_{\max} = 0.35$, and $p_{0\min} = 0.1$; and the time-varying delays $\tau_1(t) = 0.2(1 + \sin(t))$, $\tau_2(t) = 1 - 0.5\cos(t)$, $\tau_{\max} = 2$, and $\bar{\tau}_{\max} = 0.6$. The objective is to design control v_i such that the output y_i can track the desired trajectory $y_{di} = 0.5\sin(t)$, $i = 1, 2$.

The control law and adaption laws in (75)–(80) are adopted. The inputs of the NNs are $Z_1 = [s_1, x, \nu_1, \beta_1] \in R^7$ and $Z_2 = [s_2, x, \nu_2, \beta_2, v_1] \in R^8$, where $\nu_i = \lambda_i(\dot{y}_i - \dot{y}_{id}) - \dot{y}_{id}$ and $\beta_i = \dot{y}_{id} - \lambda_i(y_i - y_{id})$, $i = 1, 2$. Employing three nodes for each input dimension, we end up with 3^7 nodes for the network $\hat{W}_1^T S(Z_1)$, and 3^8 nodes for the network $\hat{W}_2^T S(Z_2)$. The bounding functions for the time-delay term are chosen as $\varrho_1(x_1(\tau)) = 0.1|x_{11}(\tau)|$ and $\varrho_2(x_2(\tau)) = 0.2|x_{22}(\tau)|$, and the following initial conditions and controller design parameters are adopted in the simulation: $x_{11}(0) = -0.4$, $x_{12}(0) = x_{21}(0) = x_{22}(0) = 0.5$, $v_1(0) = v_2(0) = 0$, $\hat{p}_1(0, r) = \hat{p}_2(0, r) = 0$, $\hat{W}_1(0) = \hat{W}_2(0) = 0$, $\Gamma_1 = \text{diag}\{1.0\}$, $\Gamma_2 = \text{diag}\{0.025\}$, $\sigma_1 = 0.2$, $\sigma_1 = 2.5$, $\eta_1 = \eta_2 = 0.01$, $\sigma_{p1} = \sigma_{p2} = 0.05$ $k_{11} = k_{21} = 0.1$, $k_{13} = k_{23} = 0.001$, $\lambda_1 = 2.5$, $\lambda_2 = 2.0$, and $c_{s_1} = c_{s_2} = 0.0001$.

Simulation results for MIMO plant S_2, as described in (101), are shown in Figs. 13–20. From Fig. 13, it is seen that good tracking performance is achieved despite large initial tracking errors e_1 and e_2, and they converge to a small neighborhood of zero in a relatively short time. At the same time, it can be observed, in Figs. 14–16, that the control signals, norms of NN weights, and states x_{12} and x_{22} remain bounded. Fig. 17 shows the nonlinear approximation capability of NNs $\hat{W}_1^T S(Z_1)$ and

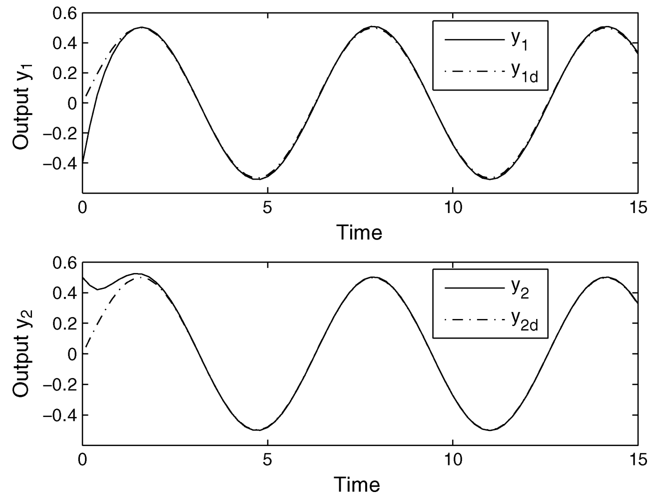

Fig. 13. Output tracking performance of MIMO plant S_2.

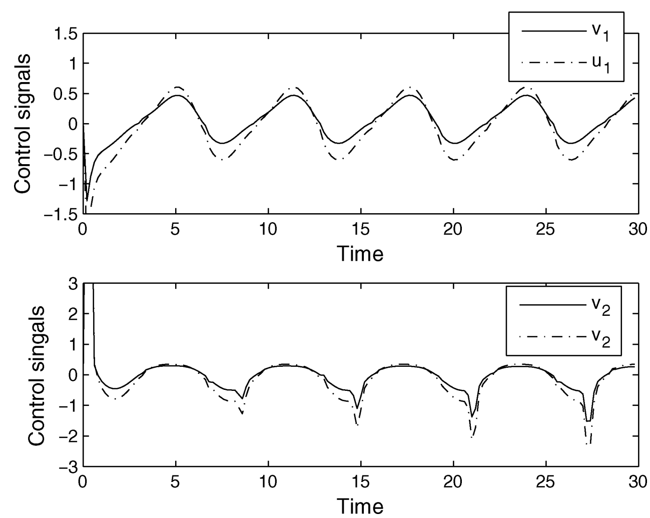

Fig. 14. Control signals of MIMO plant S_2.

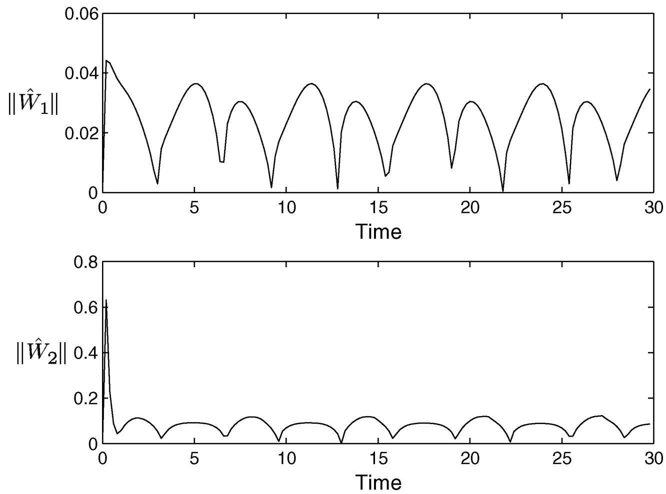

Fig. 15. Norm of NN weights of MIMO plant S_2.

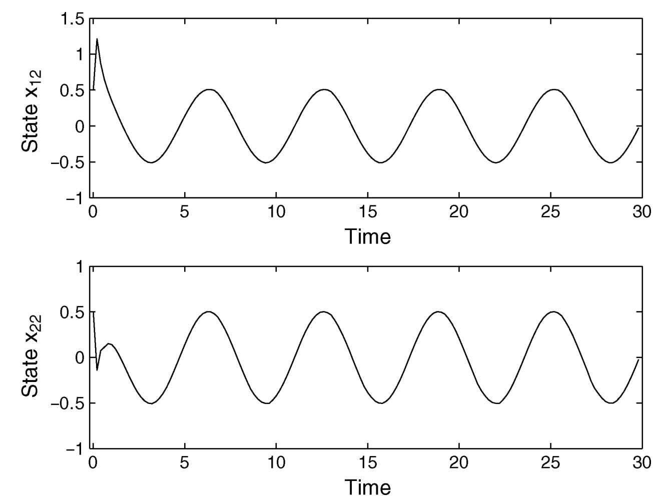

Fig. 16. Other states of MIMO plant S_2.

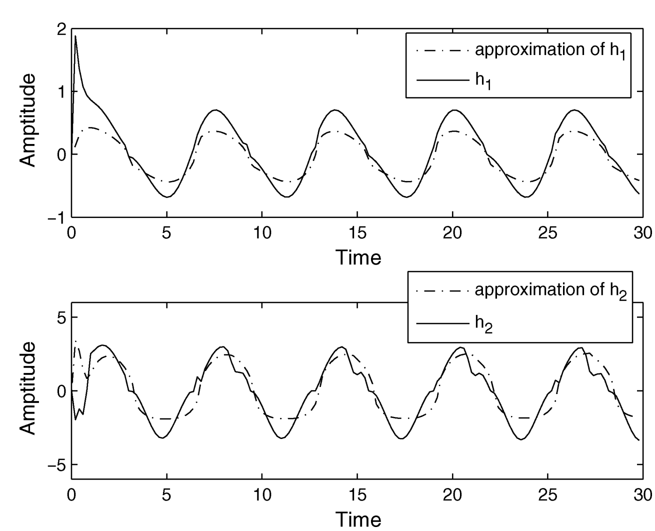

Fig. 17. Learning behavior of NNs of MIMO plant S_2.

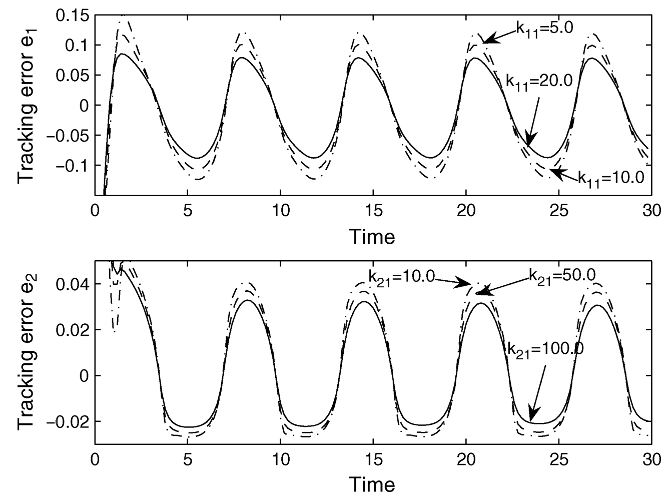

Fig. 18. Tracking error comparison result of MIMO plant S_2 for different k_{11} and k_{21}.

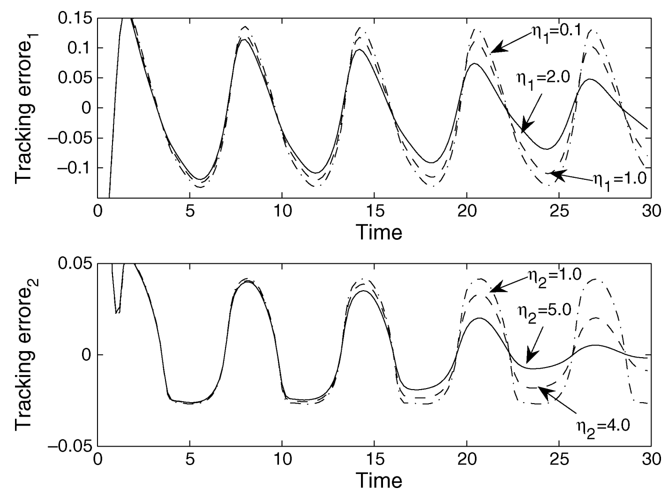

Fig. 19. Tracking error comparison result of MIMO plant S_2 for different η_1 and η_2.

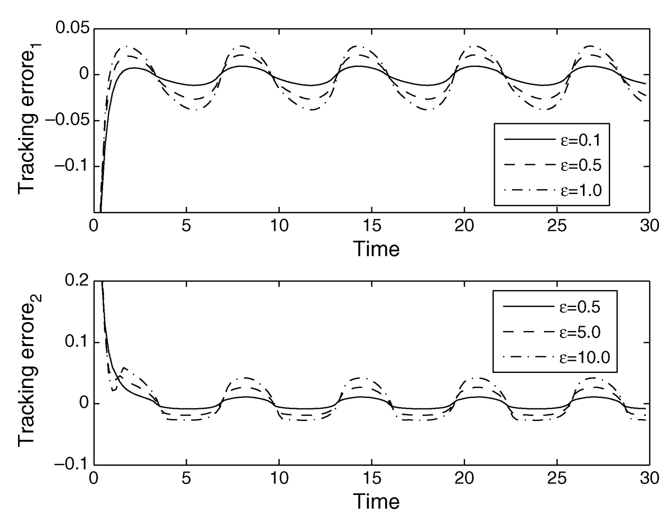

Fig. 20. Tracking error comparison result of MIMO plant S_2 for different ϵ.

$\hat{W}_2^T S(Z_2)$. Similar relationships between variations of control parameters and effects on tracking performance, as shown for the SISO case, can be verified for the MIMO case as well in Figs. 18–20.

V. Conclusion

Adaptive variable structure neural control has been proposed for a class of uncertain MIMO nonlinear systems with unknown state time-varying delays and PI hysteresis nonlinearities. The uncertainties from unknown time-varying delays have been compensated for through the use of appropriate Lyapunov–Krasovskii functionals. The effect of the unknown hysteresis with the PI models was also mitigated using the proposed control. The controller has been made to be free from singularity problem by utilizing integral Lyapunov function. Based on the principle of sliding-mode control, the developed controller can guarantee that all signals involved are SGUUB. Simulation results have verified the effectiveness of the proposed approach. As for future work, it would be interesting to extend the results reported here to deal with some applications involving hysteresis and time delays, such as smart material actuators.

ACKNOWLEDGMENT

The authors would like to thank the anonymous reviewers for constructive comments that helped to improve the quality and presentation of this paper.

REFERENCES

[1] G. Tao and P. V. Kokotovic, "Adaptive control of plants with unknown hysteresis," *IEEE Trans. Autom. Control*, vol. 40, no. 2, pp. 200–212, Feb. 1995.

[2] X. Tan and J. S. Baras, "Modeling and control of hysteresis in magnestrictive actuators," *Automatica*, vol. 40, no. 9, pp. 1469–1480, 2004.

[3] C. Y. Su, Y. Stepanenko, J. Svoboda, and T. P. Leung, "Robust adaptive control of a class of nonlinear systems with unknown backlash-like hysteresis," *IEEE Trans. Autom. Control*, vol. 45, no. 12, pp. 2427–2432, Dec. 2000.

[4] J. Zhou, C. Y. Wen, and Y. Zhang, "Adaptive backstepping control design of a class of uncertain nonlinear systems with unknown backlash-like hysteresis," *IEEE Trans. Autom. Control*, vol. 49, no. 10, pp. 1751–1757, Oct. 2004.

[5] J. W. Macki, P. Nistri, and P. Zecca, "Mathematical models for hysteresis," *SIAM Rev.*, vol. 35, pp. 94–123, 1993.

[6] C. Y. Su, Q. Wang, X. Chen, and S. Rakheja, "Adaptive variable structure control of a class of nonlinear systems with unknown Prandtl-Ishlinskii hysteresis," *IEEE Trans. Autom. Control*, vol. 50, no. 12, pp. 2069–2074, Dec. 2005.

[7] Q. Wang and C. Y. Su, "Robust adaptive control of a class of nonlinear systems including actuator hysteresis with Prandtl-Ishlinskii presentations," *Automatica*, vol. 42, no. 5, pp. 859–867, 2006.

[8] P. L. Liu and T. J. Su, "Robust stability of interval time-delay systems with delay-dependence," *Syst. Control Lett.*, vol. 33, no. 4, pp. 231–239, 1998.

[9] L. Dugard and E. Veriest, *Stability and Control of Time-Delay Systems*. Berlin, Germany: Springer-Verlag, 1997.

[10] J.-P. Richard, "Time-delay systems: An overview of some recent advances and open problems," *Automatica*, vol. 39, pp. 1667–1694, 2003.

[11] J. Hale, *Theory of Functional Differential Equations*, 2nd ed. New York: Springer-Verlag, 1977.

[12] V. B. Kolmanovskii and J. Richard, "Stability of some linear systems with delays," *IEEE Trans. Autom. Control*, vol. 44, no. 5, pp. 984–989, May 1999.

[13] S.-L. Niculescu, *Delay Effects on Stability: A Robust Control Approach*. London, U.K.: Springer-Verlag, 2001.

[14] K. Gu, V. L. Kharitonov, and J. Chen, *Stability of Time-Delay Systems*. Boston, MA: Birkhäuser, 2003.

[15] V. L. Kharitonov and D. Melchor-Aguilar, "Lyapunov-Krasovskii functionals for additional dynamics," *Int. J. Robust Nonlinear Control*, vol. 13, pp. 796–804, 2003.

[16] S. K. Nguang, "Robust stabilization of a class of time-delay nonlinear systems," *IEEE Trans. Autom. Control*, vol. 45, no. 4, pp. 756–762, Apr. 2000.

[17] S. Zhou, G. Feng, and S. K. Nguang, "Comments on robust stabilization of a class of time-delay nonlinear systems," *IEEE Trans. Autom. Control*, vol. 47, no. 9, pp. 1586–1586, Sep. 2002.

[18] S. S. Ge, F. Hong, and T. H. Lee, "Adaptive neural network control of nonlinear systems with unknown time delays," *IEEE Trans. Autom. Control*, vol. 48, no. 11, pp. 2004–2010, Nov. 2003.

[19] S. S. Ge and K. P. Tee, "Approximation-based control of nonlinear MIMO time-delay systems," *Automatica*, vol. 43, no. 6, pp. 31–43, 2007.

[20] Y. Sun, J. Hsieh, and H. Yang, "On the stability of uncertain systems with multiple time-varying delays," *IEEE Trans. Autom. Control*, vol. 42, no. 1, pp. 101–105, Jan. 1997.

[21] B. Xu and Y. Liu, "An improved Razumikhin-type theorem and its applications," *IEEE Trans. Autom. Control*, vol. 39, no. 4, pp. 839–841, Apr. 1994.

[22] M. Jankovic, "Control Lyapunov-Razumikhin functions and robust stabilization of time delay systems," *IEEE Trans. Autom. Control*, vol. 46, no. 7, pp. 1048–1060, Jul. 2001.

[23] J. Pan, C.-Y. Su, and Y. Stepanenko, "Modeling and robust adaptive control of metal cutting mechanical systems," in *Proc. Amer. Control Conf.*, Arlington, VA, 2001, pp. 1268–1273.

[24] S. S. Ge, C. C. Hang, and T. Zhang, "Adaptive neural network control of nonlinear systems by state and output feedback," *IEEE Trans. Syst. Man Cybern. B, Cybern.*, vol. 29, no. 6, pp. 818–828, Dec. 1999.

[25] M. Krstić, I. Kanellakopoulos, and P. V. Kokotović, *Nonlinear and Adaptive Control Design*. New York: Wiley, 1995.

[26] R. Sepulchre, M. Jankovic, and P. V. Kokotović, *Constructive Nonlinear Control*. London, U.K.: Springer-Verlag, 1997.

[27] R. M. Sanner and J. E. Slotine, "Gaussian networks for direct adaptive control," *IEEE Trans. Neural Netw.*, vol. 3, no. 6, pp. 837–863, Nov. 1992.

[28] M. M. Polycarpou, "Stable adaptive neural control scheme for nonlinear systems," *IEEE Trans. Autom. Control*, vol. 41, no. 3, pp. 447–451, Mar. 1996.

[29] S. Haykin, *Neural Networks: A Comprehensive Foundations*, 2nd ed. Upper Saddle River, NJ: Prentice-Hall, 1999.

[30] S. S. Ge, C. C. Hang, T. H. Lee, and T. Zhang, *Stable Adaptive Neural Network Control*. Boston, MA: Kluwer, 2002.

[31] J. A. Farrell and M. M. Polycarpou, *Adaptive Approximation Based Control*. Hoboken, NJ: Wiley, 2006.

[32] W. Lin and C. J. Qian, "Adaptive control of nonlinearly parameterized systems: The smooth feedback case," *IEEE Trans. Autom. Control*, vol. 47, no. 8, pp. 1249–1266, Aug. 2002.

[33] S. S. Ge, C. C. Hang, and T. Zhang, "A direct adaptive controller for dynamic systems with a class of nonlinear parameterizations," *Automatica*, vol. 35, no. 4, pp. 741–747, 1999.

[34] S. S. Ge, F. Hong, and T. H. Lee, "Adaptive neural control of nonlinear time-delay systems with unknown virtual control coefficients," *IEEE Trans. Syst. Man Cybern. B, Cybern.*, vol. 34, no. 1, pp. 499–516, Feb. 2004.

[35] P. Krejci and K. Kuhnen, "Inverse control of systems with hysteresis and creep," *Inst. Electr. Eng. Proc.—Control Theory Appl.*, vol. 148, no. 3, pp. 185–192, 2001.

[36] N. Hovakimyan, E. Lavretsky, and A. Sasane, "Dynamic inversion for nonaffine-in-control systems via time-scale separation. Part I," *J. Dyn. Control Syst.*, vol. 13, no. 4, pp. 451–465, 2007.

[37] T. P. Zhang and S. S. Ge, "Adaptive neural control of MIMO nonlinear state time-varying delay systems with unknown dead-zones and gain signs," *Automatica*, vol. 43, pp. 1021–1033, 2007.

[38] S. S. Ge and C. Wang, "Adaptive neural network control of uncertain MIMO nonlinear systems," *IEEE Trans. Neural Netw.*, vol. 15, no. 3, pp. 674–692, May 2004.

Beibei Ren (S'06) received the B.E. degree in mechanical and electronic engineering and the M.E. degree in automation from Xidian University, Xi'an, China, in 2001 and 2004, respectively. Currently, she is working towards the Ph.D. degree at the Department of Electrical and Computer Engineering, National University of Singapore, Singapore.

Her current research interests include neural networks, adaptive control, nonlinear control, and their applications.

Shuzhi Sam Ge (S'90–M'92–SM'99–F'06) received the B.Sc. degree from Beijing University of Aeronautics and Astronautics, Beijing, China, in 1986 and the Ph.D. degree and DIC from Imperial College, London, U.K., in 1993.

He is founding Director of Social Robotics Lab of Interactive Digital Media Institute and Professor of the Department of Electrical and Computer Engineering, National University of Singapore, Singapore. He has (co)authored three books and over 300 international journal and conference papers, and edited one book. His current research interests include social robotics, multimedia fusion, adaptive control, intelligent systems, and artificial intelligence.

Dr. Ge is the founding Editor-in-Chief of the *International Journal of Social Robotics* (Springer-Verlag). He has served/been serving as an Associate Editor for a number of flagship journals and a Book Editor of the Taylor & Francis Automation and Control Engineering Series. At IEEE Control Systems Society, he served/serves as Vice President for Technical Activities (2009–2010) and Member of Board of Governors of IEEE Control Systems Society (2007–2009).

Tong Heng Lee (M'90) received the B.A. degree (with first class honors) in engineering tripos from Cambridge University, Cambridge, U.K., in 1980 and the Ph.D. degree in electrical engineering from Yale University, New Haven, CT, in 1987.

Currently, he is Professor at the Department of Electrical and Computer Engineering, National University of Singapore, Singapore. His research interests are in the areas of adaptive systems, knowledge-based control, intelligent mechatronics, and computational intelligence. He has coauthored three research monographs and holds four patents (two of which are in the technology area of adaptive systems, and the other two are in the area of intelligent mechatronics).

Dr. Lee currently holds Associate Editor appointments in the IEEE TRANSACTIONS ON SYSTEMS, MAN, AND CYBERNETICS, the IEEE TRANSACTIONS ON INDUSTRIAL ELECTRONICS, *Control Engineering Practice* (an IFAC journal), the *International Journal of Systems Science* (Taylor and Francis, London, U.K.), and *Mechatronics* journal (Pergamon, Oxford, U.K.). He was the recipient of the Cambridge University Charles Baker Prize in Engineering and the 2004 ASCC (Melbourne) Best Industrial Control Application Paper Prize.

Chun-Yi Su (SM'99) received the Ph.D. degree in control theory and its applications from South China University of Technology, Guangzhou, China, in 1990.

Currently, he is Professor and Concordia Research Chair at Concordia University, Montreal, QC, Canada. His current research interest is in control of systems involving hysteresis nonlinearities.

Dr. Su has served on the editorial boards of several journals, including the IEEE TRANSACTIONS ON AUTOMATIC CONTROL and the IEEE TRANSACTIONS ON CONTROL SYSTEMS TECHNOLOGY. He has also severed as an organizing committee member for many conferences.